**T.C. (T.R.)**
**BOLU ABANT İZZET BAYSAL ÜNİVERSİTESİ**
**INSTITUTE OF GRADUATE STUDIES**
**DEPARTMENT OF CHEMICAL ENGİNEERING**

# A SYNTHESIS NOVEL CATALYST AND DEVELOPMENT DESIGN OF OSCILLATION BAFFLED REACTOR FOR OXIDATIVE DESULFURIZATION OF LIGHT GAS OIL

**MASTER OF SCIENCE, CHEMICAL ENGİNEERING**

**LAYTH THAMER ABDULATEEF**

**THESIS SUPERVISOR**
**Assoc. Prof. Dr. Güler Bengüsu TEZEL TANRISEVER**
**SECOND THESIS SUPERVISOR**
**Assist. Prof. Dr. Khaleel I. Hamad**

**BOLU, 1/3/2025**

# ACCEPTANCE AND APPROVAL PAGE

The thesis entitled "**A SYNTHESIS NOVEL CATALYST AND DEVELOPMENT DESIGN OF OSCILLATION BAFFLED REACTOR FOR OXIDATIVE DESULFURIZATION OF LIGHT GAS OIL**" prepared and submitted by **LAYTH THAMER ABDULATEEF** in partial fulfillment of the requirements for the degree of **Master of Science** in Department of **CHEMICAL ENGİNEERING** with unanimity vote is hereby approved. 1/3/2025

| **Jury Members** | **Signature** |
|---|---|
| Supervisor<br>Assoc. Prof. Dr. Güler Bengüsu TEZEL TANRISEVER<br>Bolu Abant Izzet Baysal University | ..... |
| Member<br>Asst. Prof. Dr. Özlem ATEŞ DURU<br>Bolu Abant Izzet Baysal University | ..... |
| Member<br>Prof. Dr. Fatma ÖZTÜRK<br>Bogazici University | ..... |

**Institute of Graduate Studies Approval**

**Prof. Dr. İbrahim KÜRTÜL**

**Director of Institute of Graduate Studies**

# ETHICAL DECLARATION

In this thesis study, which I have prepared in accordance with Bolu Abant İzzet Baysal University, Institute of Graduate Studies' Thesis Writing Guide and Template;

- I have obtained the data, information and documents presented in the thesis within the framework of academic and ethical rules,
- I have presented all information, documents, evaluations, and results in accordance with the rules of scientific ethics and morality,
- I have cited and referenced all the works I have benefited from in the thesis study,
- I have not made any changes to the data used,
- I declare that the work I have presented in this thesis is original, and in any other case, I declare that I accept all loss of rights that may arise against me.

According to the similarity report obtained by applying the filters determined by the directorate of the institute in the Turnitin program related to the thesis, the similarity index of the thesis does not exceed 30%.

……..

**LAYTH THAMER ABDULATEEF**

# ABSTRACT

**A SYNTHESIS NOVEL CATALYST AND DEVELOPMENT DESIGN OF OSCILLATION BAFFLED REACTOR FOR OXIDATIVE DESULFURIZATION OF LIGHT GAS OIL**
**MSC THESİS**
**LAYTH THAMER ABDULATEEF**
**BOLU ABANT IZZET BAYSAL ÜNİVERSİTESİ**
**INSTITUTE OF GRADUATE STUDIES**
**DEPARTMENT OF CHEMICAL ENGİNEERING**
**(SUPERVISOR: Assoc. Prof. Dr. Güler Bengüsu TEZEL TANRISEVER )**
**(CO-SUPERVISOR:Assist. Prof. Dr. KHALEEL I. HAMAD)**

**BOLU, 3 JANUARY 2025**
**XIII + 82 pages**

Sulfur compounds present in diesel fuel pose significant environmental and health concerns. This study introduces a novel approach to remove sulfur from light gas oil through oxidative desulfurization (ODS) using a mesoporous Pd/Zeolite catalyst in an oscillatory baffled reactor (OBR). A series of experiments were conducted to investigate the influence of various parameters, including temperature (40-80 °C), residence time (4-12 minutes), and oscillation frequency (0.4-1.2 Hz), on the sulfur removal efficiency. The mesoporous structure of the catalyst facilitated the adsorption and oxidation of sulfur-containing compounds. The OBR design significantly enhanced mass and heat transfer, improving sulfur removal.Under optimal conditions (80 °C, 12 minutes residence time, and 1.2 Hz oscillation frequency), a remarkable sulfur removal efficiency of 93.11% was achieved. This research provides a promising pathway towards producing cleaner and more environmentally friendly diesel fuels.

**KEYWORDS:** ODS process, OBR, palladium oxide, Zeolite, Light gas oil

# ÖZET

**HAFİF GAZ YAĞININ OKSİDATİF KÜKÜRT GİDERİMİ İÇİN YENİ KATALİZÖRLERİN SENTEZİ VE SALINIM ŞAŞIRTMALI REAKTÖRÜN GELİŞTİRME TASARIMI**
**YÜKSEK LİSANS TEZİ**
**LAYTH THAMER ABDULATEEF**
**BOLU ABANT IZZET BAYSAL ÜNİVERSİTESİ**
**LİSANSÜSTÜ EĞİTİM ENSTİTÜSÜ**
**KİMYA MÜHENDİSLİĞİ ANA BİLİM DALI**
**(TEZ DANIŞMANI: DOÇ. Dr. Güler Bengüsu TEZEL TANRISEVER**
**(İKİNCİ DANIŞMAN: DOÇ. Prof. Dr. KHALEEL I. HAMAD )**
**BOLU, 3 OCAK 2025**
**XIII + 82 pages**

Dizel yakıtlardaki kükürt bileşikleri, çevre ve insan sağlığı için önemli bir tehdit oluşturmaktadır. Bu çalışma, hafif gaz yağından kükürtün oksidatif desülfürizasyonu (ODS) için osilasyonlu engelli bir reaktörde (OBR) yeni bir mezo gözenekli Pd/Zeolite katalizörü kullanarak yenilikçi bir yaklaşım sunmaktadır.Çeşitli sıcaklık (40-80 °C), kalış süresi (4-12 dakika) ve osilasyon frekansı (0.4-1.2 Hz) parametrelerinin kükürt giderim verimi üzerindeki etkilerini incelemek için bir dizi deney gerçekleştirilmiştir. Mezo gözenekli yapısı sayesinde katalizör, kükürt bileşiklerinin adsorpsiyonunu ve oksidasyonunu kolaylaştırmıştır. OBR tasarımı, kütle ve ısı transferini önemli ölçüde artırarak kükürt giderimini iyileştirmiştir. Optimal koşullar altında (80 °C, 12 dakika kalış süresi ve 1.2 Hz osilasyon frekansı), %93.11 gibi dikkat çekici bir kükürt giderim verimi elde edilmiştir. Bu çalışma, daha temiz ve çevre dostu dizel yakıtlarının üretimi için umut verici bir yol sunmaktadır.

**ANAHTAR KELİMELER:** Oksidatif desülfürizasyon, hafif gaz yağı, mezo gözenekli katalizör, osilasyonlu engelli reaktör, kükürt giderimi, çevresel etki.

# TABLE OF CONTENTS

**Page**

# LIST OF FIGURES

**Page**

# LIST OF TABLES

**Page**

# LIST OF ABBREVIATIONS AND SYMBOLS

**ADS** : Adsorption desulfurization process
**BDS** : Bio-Desulfurization
**BET** : Brunauer-Emmett Teller
**DBT** : Dibenzothiophene
**EDS** : Extraction desulfurization
***f*** : Oscillation frequency (Hz)
**FESEM** : Field emission Scanning Electron Microscopy
**FTIR** : Fourier transform infrared
**HDS** : Hydrodesulfurization
**$H_2O_2$** : Hydrogen peroxide
**IWI** : Incipient Wetness Impregnation
**KLa** : Coefficient of total mass transfer
***l*** : Baffle spacing (mm)
**LGO** : Light gas oil
**LHSV** : Liquid hour space velocity
**OBR** : Oscillatory baffled reactor
**ODS** : Oxidative desulfurization
**OSCs** : Organic sulfur compounds
**ppm** : Part per million
**SA** : Surface area ($m2.g^{-1}$)
**τ** : Residence time (min)
**TBR** : Trickle bed reactor
**TGA** : Thermogravimetric
**XRD** : X-ray diffraction
**4-MDBT** : 4-methydibenzothiophene
**4,6-DMDBT:** 4,6-di-methyl di-benzothiophene
**4,6-DEDBT:** 4,6-di-ethyl di-benzothiophene
**DI** : dry impregnation

# ACKNOWLEDGEMENT

First of all, I thank Allah Almighty for everything, who helped me overcome the difficulties I faced in this study until I reached this stage.

I would like to extend my sincere thanks and deep gratitude to my supervisor **Assoc. Prof. Dr. GÜLER BENGÜSU TEZEL** for allowing me to conduct this research and for her supervisory guidance and constructive suggestions that were very useful to me in my research career. Also, thanks and appreciation are extended to my Co-supervisor **Dr. KHALEEL I. HAMAD** who helped me overcome many obstacles and problems and provided useful advice and suggestions during the research work.

I thank **Prof. Dr. TURGAY PEKDEMIR**, Head of the Chemical Engineering Department, and I also thank all the staff of the Chemical Engineering Department.

I would also like to a special thanks to the examining committee members for their efforts and patience and their invaluable comments on my thesis.

To the dear and precious one who passed away before I completed this work **MY FATHER**: You will remain in my heart and memory, if it were not for God's grace and then your grace and constant support for me, I would not have reached where I am now. I ask Allah Almighty to have mercy on you and unite me with you in heaven.

Finally, I extend my deepest thanks and appreciation to my mother, brothers and sisters, wife, friends and relatives for their patience, prayers and encouragement, They played the biggest role in overcoming all the difficulties.

# 1. INTRODUCTION

## 1.1 Background

Energy is a significant concern in economic development, given that nature and society have an important relationship, energy plays a major role in this relationship (Chen et al., 2013). The world's largest and most widely used energy source to date is crude oil, as the fuel used in diverse transportation, such as diesel, gasoline, and jet fuel, occupies the largest part of crude oil derivatives (Al-Malki, 2004).

Oil and gas are still expected to meet up to 50% of universal energy demand until 2050, despite continued encouragement of renewable and sustainable energy sources and expansion in the diversity of their production methods (Adam et al., 2021), as shown in Figure 1.1 below.

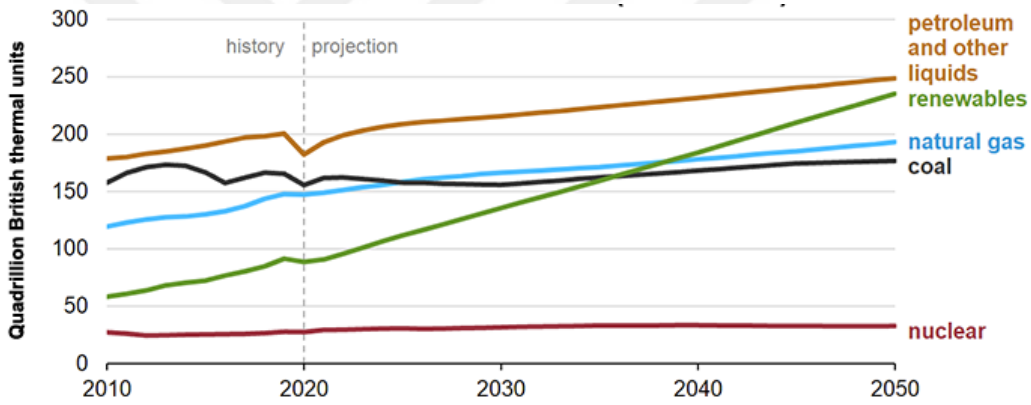


**Figure 1.1.** Global energy consumption (Zhongming et al., 2021)

Such crudes and their derivatives contain sulfur. The sulfur content and specific gravity according to the American Petroleum Institute (API gravity), are two properties that have a significant impact on the value of crude oil (M. N. Abbas & Ibrahim, n.d.). The indicators tend to rise for pollution associated with the use of petroleum derivatives in addition to pollution resulting from the extraction and refining of crude oil (Campos-Martin & Capel-Sanchez, 2021).

There is a large group of sulfur compounds in gas oil, which can be categorized into four main groups: mercaptans, thiophenes, sulfides, and disulfides. These groups are considered a major priority for fuels derived from crude oil, as

they are one of the most dangerous environmental pollutants of petroleum and its derivatives (Campos-Martin & Capel-Sanchez, 2021).

Sulfur is found in fossil fuels naturally as various organic and inorganic compounds, and regrettably, burning fossil fuels to produce energy is the prevailing modern technology so far. Sulfur oxide gases are formed when sulfur oxidized during the process. These formed gases react with water and air in atmosphere pressure to produce toxic sulphates, causing air and water pollution and the formation of acid rain that damages vegetation, crops and changes the soil makeup, which affects the natural diversity of plants and animals, which ultimately leads to environmental instability (ARP, 2010). It also causes health problems such as trigger asthma and respiratory diseases (Gokhale & Khare, 2004).

Moreover, the organic sulfur compounds in crude oil and its derivatives are the cause of many industrial process problems such as corrosion of pumps, refining equipment and their transport pipes, premature failure of combustion engines, and the deactivation and poisoning of catalysts used in refining industries (Saleh, 2020).

Therefore, environmental concerns have prompted the need to remove sulfur-containing compounds from gas oil and other derivatives (Zhao et al., 2003). New stringent environmental regulations have drawn attention to the process of desulfurization of fuels, with the permissible limit of sulfur reaching 15 ppm in the United States, while the limit set by the European Union and China is 10 ppm. Therefore, the process of ultra-deep desulfurization of petroleum derivatives has recently begun to receive great attention, as the effort in this area also aims to meet the limited supply of sulfur-free fuel (>1 ppm) used in fuel cells, not only to implement the requirements of new stringent environmental regulations (Shafiq et al., 2021). In addition to providing environmentally friendly fuel, the global demand for which has recently begun to increase (Ismagilov et al., 2011).

To obtain environmentally friendly fuel, and due to the difficulty of reducing sulfur in fuel to (< 10 ppm) using the hydrogen hydrodesulfurization process (HDS), which is the prevailing traditional method, as it is a process that requires high operating costs and harsh operating conditions for the HDS reactor, whose temperature ranges between 300 - 450 °C and pressure ranges from 35 - 270 bar, and high hydrogen consumption depending on the feed and the required level

of desulfurization (Rezvani et al., 2021). In addition to losing the octane rating of the fuel treated under these conditions due to the hydrogenation of olefins and their transformation into recombinant mercaptans after their reaction with $H_2S$, thus increasing hydrogen consumption (Shiflett & Krenzke, 2002).

The conventional hydrodesulfurization (HDS) process, although historically dominant, has become increasingly cost-prohibitive due to stringent fuel specifications. This has necessitated the exploration of alternative desulfurization technologies. Oxidative desulfurization (ODS) has emerged as a promising alternative, offering several advantages: high efficiency, mild reaction conditions, and lower operational costs. The reduced complexity of ODS processes allows for simpler equipment and lower capital investment, making it a more economically viable option compared to HDS (Gao et al., 2018).

The oxidative desulfurization process has great advantages over the hydrodesulfurization process, as the former can react with all sulfur compounds present in the fuel and reduce them, which are difficult to reduce in the hydrogen removal process (Otsuki et al., 2000). In contrast, to provide an effective and observable catalytic desulfurization process with a longer operating life, great efforts must be made to select a selective and effective catalyst for this process (Sharifi et al., 2018)(Dardouri et al., 2019).

A suitable reactor must be chosen to assess the efficacy of the newly developed catalyst and consider its commercial viability within an integrated fuel desulfurization process. The oscillatory baffled reactor (OBR) presents an innovative solution in tubular reactor design. It has been shown to significantly enhance mass and heat transfer rates compared to traditional tubular reactors, making it an ideal candidate for advanced oxidation processes, where these factors are crucial (Humadi et al., 2021).

## 1.2 The Sulfur

Sulfur compounds are significant non-hydrocarbon components found in petroleum, existing in various structural forms. Heavy fractions and residuals derived from crude oil processing contain a substantial amount of these sulfur compounds (Speight, 2000). While the significance of sulfur compounds in petroleum may not be immediately apparent, their presence has detrimental consequences.

In finished petroleum products like gasoline, sulfur compounds can lead to engine corrosion, particularly during winter conditions when water containing sulfur dioxide accumulates in the crankcase. Additionally, mercaptans, a specific type of sulfur compound, can cause corrosion of copper and brass when exposed to air and negatively impact the color stability of gasoline and other liquid fuels (Babich & Moulijn, 2003; C. Song, 2013; Song & Ma, 2003).

The distribution of sulfur compounds in crude oils has been extensively studied since the 1890s, allowing for the identification of various general patterns. The proportion of sulfur increases with the boiling point of the crude oil fraction. Excessive temperature during distillation can lead to the thermal decomposition of high molecular-weight sulfur compounds. Consequently, the middle fractions will have a higher concentration of sulfur compounds compared to the higher-boiling fractions. The distribution of different types of sulfur compounds significantly varies among crude oils from various origins. While it is difficult to definitively link specific trends to the occurrence of compound types in different crude oils, a general observation can be made: as the boiling point of fractions from a particular crude oil increases, the sulfur content tends to rise (Shiflett & Krenzke, 2002).

## 1.3 Organic sulfur compounds found in crud oil distillates and it's oxidation reactions

### 1.3.1 Categories of Sulfur in petroleum distillates

In crude oil derivatives, sulfur can be considered the only heterogeneous atom that can be found in these derivatives. Different types of sulfur are distributed in different proportions among crude oil derivatives depending on the origin of the

crude oil from different sources (Nawaf, 2015). The Table 1.1 illustrated below, the popular varieties of sulfur compounds found in liquid fuels.

**Table 1.1.** The most found sulfur types in liquid fuels (Song & Ma, 2003)

| Type | Structure | Boiling point (°C) | Reactivity | Fuel range |
|---|---|---|---|---|
| Mercaptans | 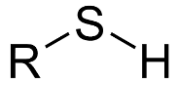 | - | Fast | Gasoline |
| Sulfides | 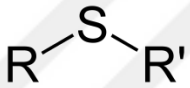 | - | Moderately | Gasoline |
| Thiophenes | 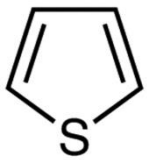 | 85 | Weak | Gasoline, Kerosene and jet fuel |
| Benzothiophenes | 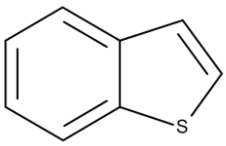 | 223 | Very weak | Gasoline, Kerosene jet fuel and Diesel |
| Dibenzothiophenes | 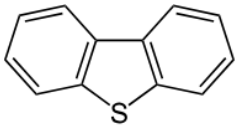 | 400 | Very weak | Diesel |

### 1.3.2 The reactions involve sulfur compounds

A significant number of studies have been published regarding the ODS process (Bagherzadeh & Amini, 2009; Di Giuseppe et al., 2009; Xia et al., 1999), focusing on various types of organic sulfur compounds such as mercaptans, sulfides, and thiophenes. The chemical reactions of these organic sulfur compounds (OSCs) that take place in the ODS process can be summarized as follows:

- Mercaptan undergoes direct oxidation to form disulfide (Xia et al., 1999):

  $$\boldsymbol{RSH + Oxidant \rightarrow RSSR}$$

- Sulfide undergoes oxidation to form sulfone, which subsequently oxidizes to yield sulfoxide (Bagherzadeh & Amini, 2009):

  $$\boldsymbol{RSR + Oxidant \rightarrow RSRO + Oxidant \rightarrow RSRO_2}$$

- Thiophenes undergo oxidation to form thiophene sulfone, followed by further oxidation to yield thiophene sulfoxide (Di Giuseppe et al., 2009):

  $$\boldsymbol{Th + Oxidant \rightarrow ThO + Oxidant \rightarrow ThO_2}$$

  $$\boldsymbol{BT + Oxidant \rightarrow BTO + Oxidant \rightarrow BTO_2}$$

  $$\boldsymbol{DBT + Oxidant \rightarrow DBTO + Oxidant \rightarrow DBTO_2}$$

## 1.4 Classification of Desulfurization Technologies

The sulfur concentration in fuels, the function of hydrogen, the type of process (chemical or physical), and the economic cost are common variables in the classification of desulfurization processes inside refineries. Desulfurization methods for treating organic sulfur compounds can be categorized into three groups: decomposed, separated without decomposition, or both separated and then decomposed, as illustrated in Figure 1.2 (“A Review on Desulfurization Techniques of Liquid Fuels,” 2016).

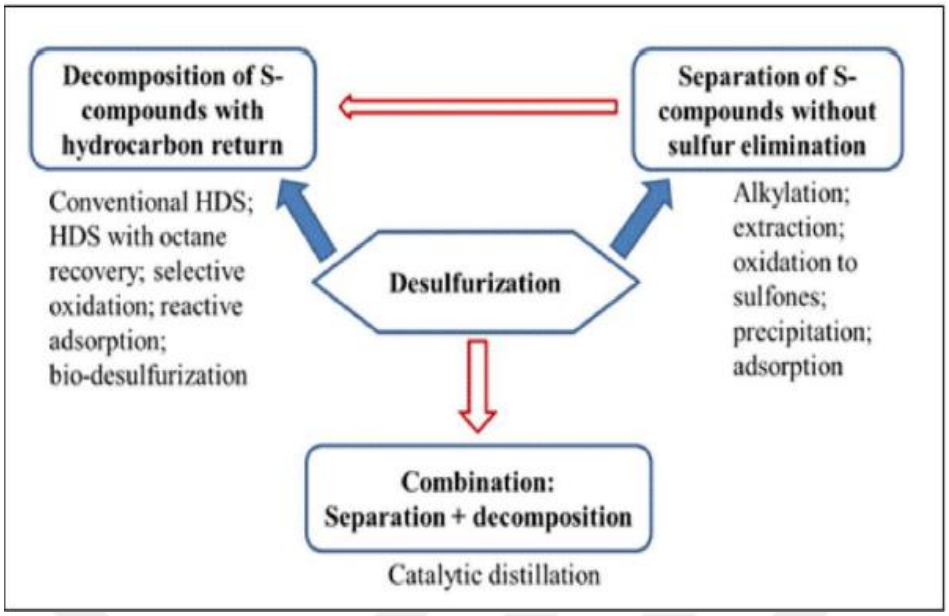


**Figure 1.2.** Classification of Desulfurization Processes in the Refineries ("A Review on Desulfurization Techniques of Liquid Fuels," 2016)

Conventional Hydrodesulfurization (HDS) is the primary technique for decomposing sulfur compounds into hydrogen sulfide, which is subsequently extracted from the hydrogen stream. In the second approach (i.e., ODS), sulfur compounds are either separated or initially converted into more easily separable compounds (i.e., sulfones) through the use of an oxidant. The third technique involves separating organic sulfur compounds from crude oil and subsequently thermally or catalytically decomposing them in a specialized unit (D. Liu et al., 2010).

Figure 1.3 illustrates the two primary categories of desulfurization processes: Hydrodesulfurization (HDS) and non-Hydrodesulfurization. These categories are distinguished by their use of hydrogen. HDS-based processes rely heavily on hydrogen to break down sulfur compounds, while non-HDS processes operate without the use of hydrogen (Hern et al., 2020).

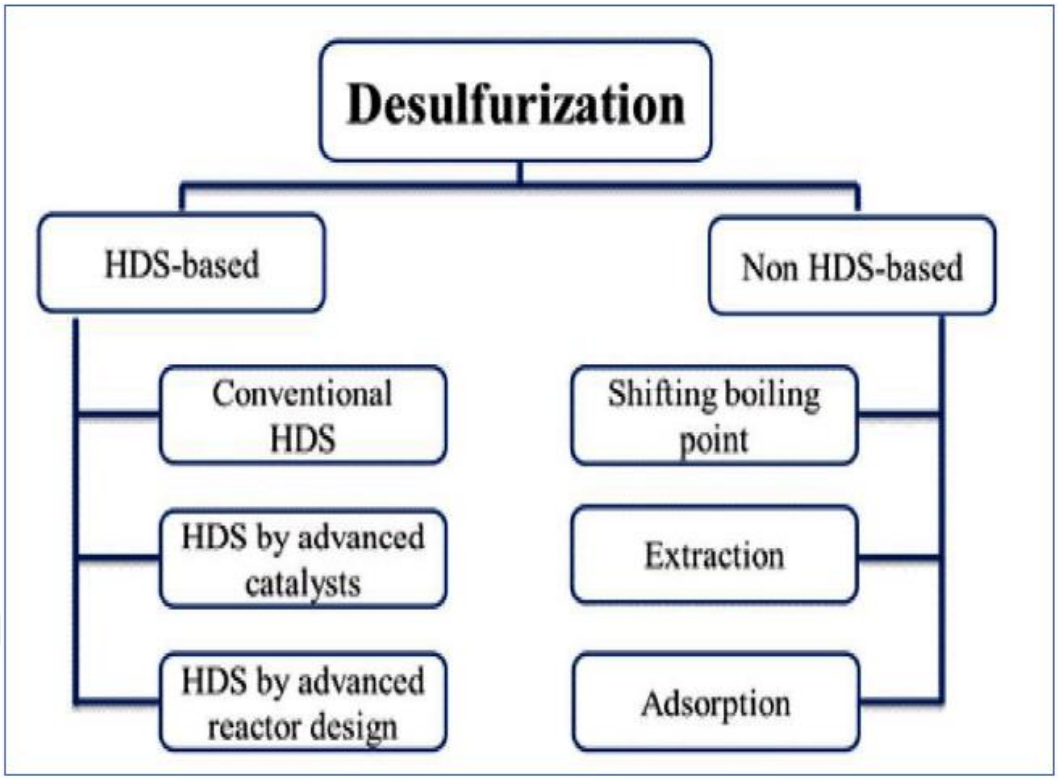


**Figure 1.3.** Classification According to the Role of Hydrogen Used in the Process("A Review on Desulfurization Techniques of Liquid Fuels," 2016)

### 1.4.1 Traditional Approaches of Hydrodesulfurization (HDS)

Hydrodesulfurization (HDS) is a catalytic hydrogenation process used to remove sulfur, nitrogen, metals, oxygen, and other undesirable elements from fuels. This process involves breaking down sulfur compounds into hydrogen sulfide, which requires the use of hydrogen. Some of these contaminants can negatively impact equipment, catalysts, and product quality (Ogunlaja, 2013).

The HDS reaction takes place in a fixed-bed reactor under elevated temperatures ranging from 300 to 400 °C and high pressures between 30 and 130 atm. Furthermore, various metals such as Co-Mo, Ni-Mo, and Ni-W, when supported on $Al_2O_3$, serve as catalysts. These catalysts offer a surface for the adsorption, dissociation, and reaction of hydrogen molecules with sulfur, resulting in the removal of hydrogen sulfide ($H_2S$) (D. Liu et al., 2010).

During the HDS process of thiophene compounds, two distinct pathways were proposed: the hydrogenolysis pathway and the hydrogenation pathway. In the hydrogenolysis pathway, the C-S bonds in organic sulfur compounds are cut off, whereas in the hydrogenation pathway, the ring undergoes hydrogenation for

saturation, followed by the removal of the sulfur atom (Silva et al., 2021). The reaction conditions, the characteristics of the sulfur compound, and the type of catalyst represent the primary constraints on the selectivity of the two pathways. At times, both pathways may occur simultaneously, utilizing distinct active sites on the catalyst surface. In the case of hydrogenolysis, the Co-Mo/$Al_2O_3$ catalyst is favored, while the Ni-Mo/$Al_2O_3$ catalyst demonstrates high activity for hydrogenation (Shafi & Hutchings, 2000). Concerning the nature of sulfur compounds, dibenzothiophene (DBT) mostly undergoes reaction via the hydrogenolysis pathway, while both hydrogenolysis and hydrogenation pathways are employed to eliminate 4,6-dimethyldibenzothiophene (4,6 DMDBT) under identical reaction conditions (Sanyangare, 2016).

A number of sulfur compounds, such as thiols, sulfides, thiophene, alkyl-thiophenes, and benzothiophene, have been thoroughly investigated using the use of HDS. Figure 1.4 shows that the reactivity of sulfur compounds has been dramatically reduced from mercaptans to alkyl-derived dibenzothiophenes as the number of rings and methyl substituents has increased (Rivera et al., 2014).

The disadvantages of the HDS process are primarily attributed to high pressure, extreme temperatures, toxic gases, and the complexity of catalytic processes (Bhadra & Jhung, 2019). The efficiency of the HDS process can be enhanced through the utilization of novel catalysts, specifically Pt-Pd/amorphous silica-alumina (Pt-Pd/ASA), alongside improved reactor designs. Severe operating conditions and advanced reactors increase the cost of the process(Blanco-Brieva et al., 2010; Huirache-Acuña et al., 2012).

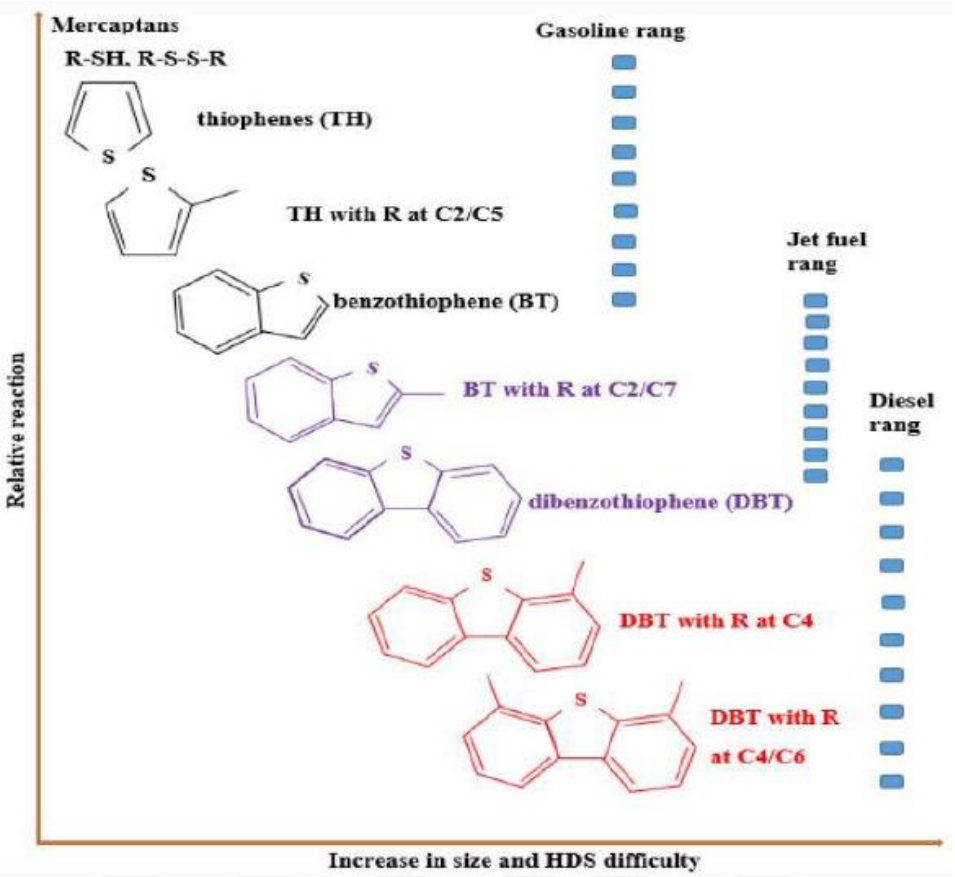


**Figure 1.4.** Classification Based on the Transformation of Sulfur Compounds ("A Review on Desulfurization Techniques of Liquid Fuels," 2016)

### 1.4.2 Alternative Technologies Not Based on HDS

Five types of technologies catalyze the decomposition of organic sulfur compounds without the need of hydrogen:

#### 1.4.2.1. Extraction-Based Desulfurization

The extraction of sulfur compounds from fuel oil, known as extractive desulphurization, relies on the principle that sulfur compounds exhibit greater solubility than hydrocarbons in a suitable solvent. Figure 1.5 illustrates the overall process flow sheet. The primary advantage of the extractive desulphurization process lies in its effectiveness under low temperature and low pressure conditions. The procedure has no effect on the chemical composition of fuel oil components. To enhance the efficiency of the separation process, it is essential to select the solvent with precision, ensuring it meets various critical requirements. The solubility of the sulfur compounds in the solvent is of utmost importance.

The solvent should possess a boiling point distinct from that of the sulfur-containing compounds, and it needs to be cost-effective to guarantee the economic viability of the process. A variety of solvents have been explored, including acetone, ethanol (Aida, 1998), polyethylene glycols (Horii et al., 1993), and nitrogen-containing solvents (Aida & Funakoshi, 1993). A desulphurization level ranging from 50% to 90% sulfur removal has been documented, depending upon the number of extraction cycles employed.

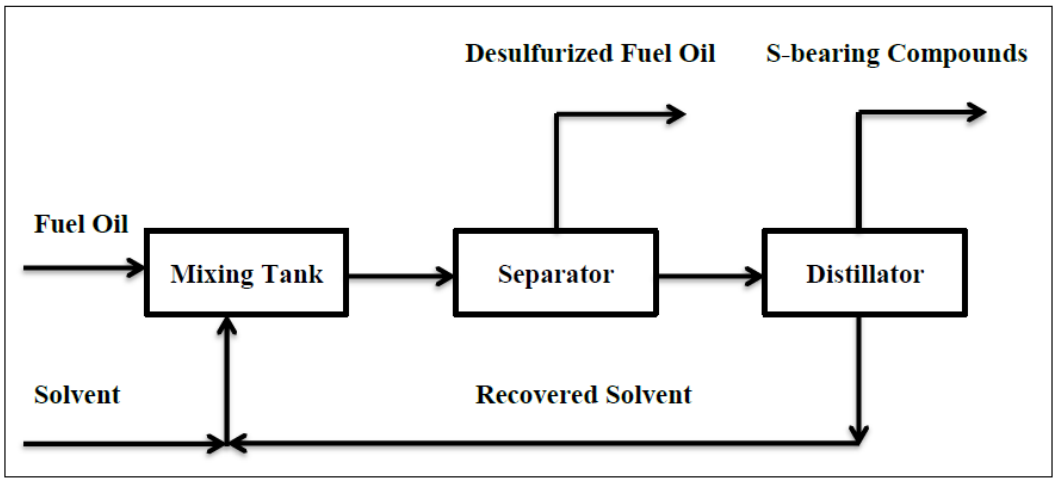


**Figure 1.5.** Overview of the extractive desulphurization process flow

The effectiveness of extractive desulphurization is primarily constrained by the solubility of organic sulfur compounds within the solvent. The selection of an appropriate solvent, considering the characteristics of the sulfur compounds targeted for removal, can significantly enhance solubility. This is typically accomplished by formulating a 'solvent cocktail' like a combination of acetone and ethanol or a mixture of tetraethylene glycol and methoxytriglycol (Aida & Funakoshi, 1993; Nawaf, 2015). The preparation of this 'solvent cocktail' presents significant challenges and is inherently inefficient, as its composition is heavily influenced by the variety of organic sulfur compounds found in the feed stream.

#### 1.4.2.2. Adsorptive Desulfurization:

Desulphurization through adsorption (ADS) relies on the capacity of solid adsorbents to selectively capture organic- sulfur compounds from refinery streams. According to the mechanism by which sulfur compounds interact with the adsorbent, ADS can be categorized into two distinct groups: adsorptive

desulphurization and reactive adsorption desulphurization. Adsorptive desulphurization relies on the physical adsorption of organic-sulfur compounds onto the surface of solid adsorbents. Regeneration typically involves the process of flushing the exhausted adsorbent with a solvent, which leads to the production of waste containing a high concentration of organic-sulfur compounds (Nanoti et al., 2011; Sarda et al., 2012).

Reactive adsorption desulfurization involves the chemical interaction between organic sulfur compounds and the adsorbent. Sulfur typically undergoes adsorption, primarily in the form of sulfide, resulting in the release of sulfur-free hydrocarbons into the purified fuel stream. The regeneration of the spent adsorbent leads to the removal of sulfur in the form of $H_2S$, S, or sulfur oxides, contingent upon the specific process utilized. The effectiveness of desulfurization is primarily influenced by the characteristics of the adsorbent, including its capacity for adsorption, selectivity towards organic-sulfur compounds, as well as its durability and ability to be regenerated (Nanoti et al., 2011; Sarda et al., 2012).

The adsorptive desulfurization method makes use of a variety of established porous solid materials as adsorbents, including activated carbon, zeolite, alumina, silica, montmorillonite activated clay, and various metal-based adsorbents (Sarda et al., 2012). The primary drawback of these processes lies in the thermal swing necessary for high-temperature regeneration or the need for an additional separation process to recover the solvent for recycling (Nanoti et al., 2011).

#### 1.4.2.3. Biological desulfurization (BDS):

This method utilizes microorganisms, including bacteria, for the removal of organosulfur compounds. Biodesulfurization (BDS) has been investigated as a substitute for hydrodesulfurization (HDS) in the extraction of organic sulfur from fuels. BDS employs bacteria as a catalyst for the removal of sulfur from fuel. In the BDS process, organosulfur compounds, including DBT and various other organic sulfur compounds, undergo oxidation by genetically modified microbes through a selective oxidative pathway, resulting in the removal of sulfur as sulfate salts (Monticello, 2000).

There are two primary methods for the BDS of alkyl-DBTs. Most attention is focused on the 4S pathway of certain bacterial species, which can effectively remove sulfur from dibenzothiophene (DBT) and its derivatives, particularly the

challenging compound 4,6-dimethyldibenzothiophene (4,6-DMDBT), which is resistant to hydrodesulfurization (HDS). Figure 1.6 illustrates that the enzymes involved in the 4S pathway of DBT can selectively target the sulfur atom while leaving the carbon content of fuels unassimilated. In this pathway, DBT undergoes a stepwise oxidation to form DBT sulfoxide, which is subsequently oxidized to DBT sulfone, and ultimately converted to 2-hydroxyl biphenyl (HBP) (Monticello, 2000).

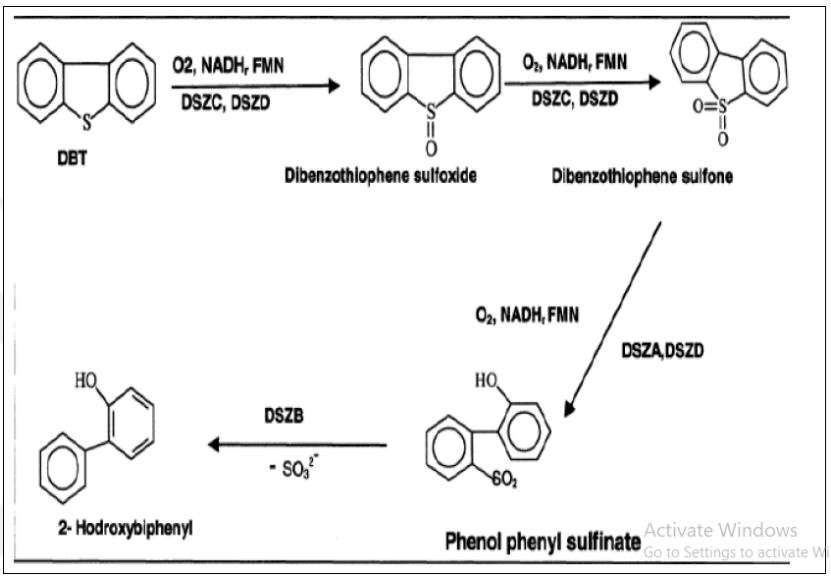


**Figure 1.6.** Pathways of Biodesulfurization (Monticello, 2000)

The complete biodiesel desulfurization of hydrodesulfurized diesel fuel resulted in a 67% decrease in total sulfur, reducing it from 1850 ppm to 615 ppm. Notably, the sulfur content of 615 ppm cannot be further diminished. For biodesulfurization to be commercially viable, it must effectively eliminate sulfur from fuels. While extensive studies have been conducted on the desulfurization of model compounds through the sulfur selective oxidative pathway, there is a paucity of published information regarding the desulfurization of fuel oils (Folsom et al., 1999; Kilbane, 2017).

#### 1.4.2.4. Desulfurization by precipitation

Desulfurization via precipitation relies on the generation and extraction of subsequent insoluble change-transfer complexes. Preliminary experiments were conducted on a model organic-sulfur compound (4, 6-DMDBT) in hexane and gas

oil, utilizing 2,4,5,7-tetranitro-9-fluoren (TNF) as the most effective π–acceptor. A suspension of the π-acceptor and sulfur-containing gas oil was agitated in a batch reactor, resulting in the formation of insoluble change-transfer complexes between the π-acceptor and DBT derivatives. The sequential procedures involve filtration to eliminate the complex generated from gas oil and the recovery of the excess π-acceptor utilizing a solid adsorbent. The current efficiency is significantly low. One treatment achieves the removal of merely 20% of the sulfur present. Additionally, competition exists in complex formation between DBT compounds and other non-sulfur aromatics, leading to reduced selectivity for DBT removal (Groysman, 2017; Vellingiri et al., 2016).

#### 1.4.2.5. Oxidative desulfurization (ODS)

Meeting the new stricter sulfur specifications requires an approach that integrates new process options with the conventional HDS process to achieve economic viability. Oxidative desulfurization (ODS) involves the conversion of sulfur compounds into their oxidized forms, specifically sulfones, serving as an alternative method for reducing sulfur content in transportation fuels. The application of the ODS process to sulfur compounds in middle distillates appears to be economically advantageous for multiple reasons (Ali et al., 2009). One of the reasons is that under mild reaction conditions, such as temperatures ranging from room temperature to 200 °C and pressures between 1 bar and 15 bar, the oxidation reaction typically leads to reduced capital investment and operational costs. Additionally, another reason is that the ODS presents an appealing option because of the increased reactivity of aromatic sulfur compounds, especially alkylated DBTs, which pose challenges in being eliminated in low-pressure hydrotreating systems. The varying reactivities stem from the increased electron density at the sulfur atom, attributed to its integration within an electron-rich aromatic framework. This effect is further amplified by the presence of alkyl groups, which are electron-donating. Consequently, larger aromatic systems and alkyl substituents enhance the likelihood of an electrophilic attack by an oxidant. Consequently, sulfur molecules that are resistant in HDS, like 4,6-DMBT, are expected to undergo favorable reactions in ODS (Ismagilov et al., 2011; ISODA, 1998). Figure 1.7 represent the optimal reaction for DBTs (Nawaf, 2015)

When compared to their unoxidized counterparts, oxidized sulfur compounds have much higher boiling points, molecular weights, and polarities. Therefore, polar solvents such acetonitrile, N-methyl pyrrolidone (NMP), dimethylformamide (DMF), and methanol enhance the solubility of sulfoxides or sulfone molecules (Akopyan et al., 2020).

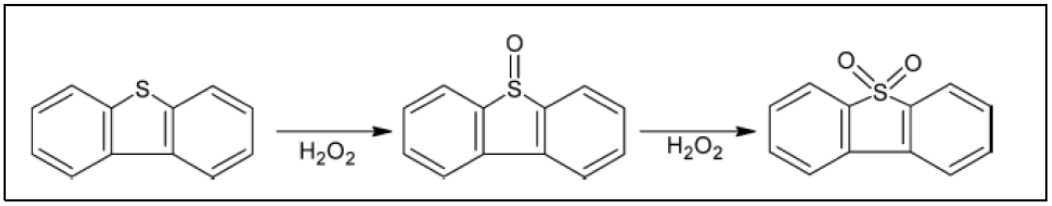


**Figure 1.7.** The optimal reaction for DBTs(Nawaf, 2015)

**The ODS process consists of two distinct stages:**

- Initially, in the context of electrophilic addition reactions, aromatic sulfur compounds present in fuels undergo oxidation to generate hexavalent sulfur (sulfones) through the incorporation of oxygen atoms.
- In the second stage, the separation of oxidized sulfur-containing compounds, such as sulfoxides or sulfones, from fuel is achieved through methods like solvent extraction, distillation, or adsorption, as illustrated in Figure 1.8 (Rajendran et al., 2020).

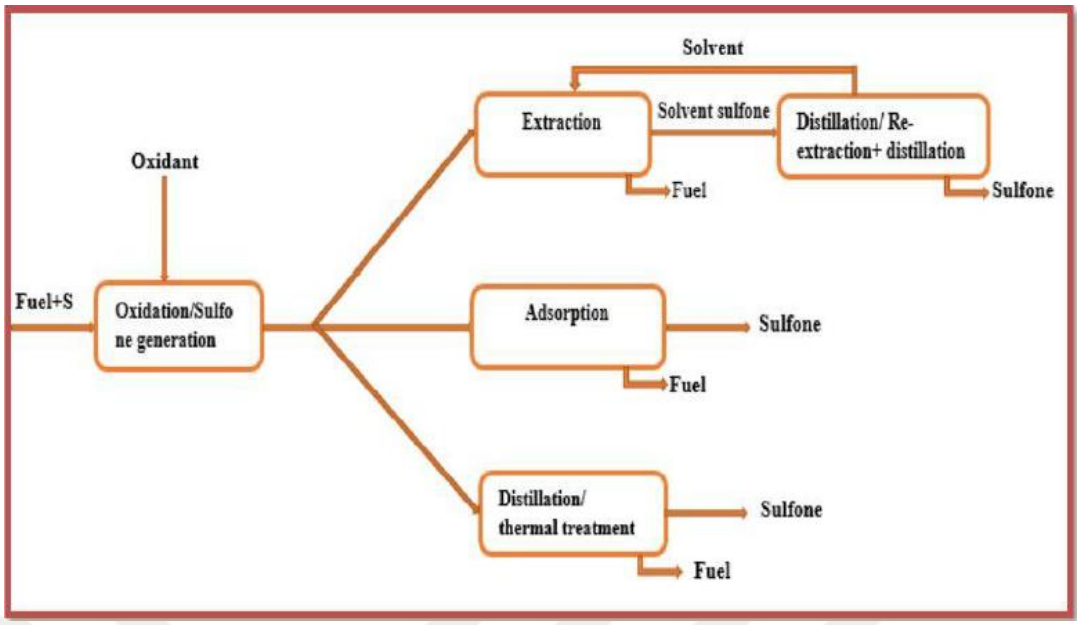


**Figure 1.8.** The Oxidative Desulfurization Reaction (Rajendran et al., 2020)

The implications, operating conditions, and risks associated with HDS and ODS processes are summarized in Table 1.2.

**Table 1.2.** HDS vs. ODS Process Comparison

| ITEM | HDS | ODS |
|---|---|---|
| Catalyst | Solid phase | Solid or liquid phase |
| Reaction type | Reduction reaction | Oxidation reaction |
| Construction expenses | Higher | Minimal |
| Pressure | Between 30 - 275 bar | Almost atmospheric pressure |
| Temperature | Elevated temperature (200-500 °C) | Almost (25-100 °C) |
| Risk | A higher risk | A lower risk |
| Cracking of feedstock | Cracking happens | No Cracking happens |
| Pollution | Contributes to air pollution through hydrogen sulfide ($H_2S$) | Environmentally friendly and safe |

## 1.5 Oxidant Types

The primary goal of the desulfurization process is to oxidize organic sulfur compounds into their corresponding sulfones and sulfoxides. To achieve this, an

oxidant is essential. An oxidant is a chemical compound that transforms organic compounds into more polar oxidized species. The selection of an appropriate oxidant for the desulfurization process is primarily influenced by factors such as active oxygen content, by-product nature, selectivity, cost, and environmental impact. Numerous oxidants have been investigated in the literature, with the most common ones summarized in Table 1.3.

**Table 1.3.** The active oxygen content and the by-products of various common oxidants (Cheng, 2008; Nawaf, 2015; Wan, 2006).

| **Oxidant type** | **activated oxygen content (%)** | **reaction's byproduct** |
|---|---|---|
| Oxygen | 100 | $H_2O$ |
| hydrogen peroxide | 47 | $H_2O$ |
| Ozone | 33 | $O_2$ |
| Nitric Acid | 25 | NOx |
| Sodium hypochlorite | 21 | NaCl |
| tert-Butyl hydro peroxide | 17 | t-BuOH |

$H_2O_2$ is a crucial oxidizing agent in the ODS process due to its strong chemical reactivity, availability, and active oxygen concentration (47%). No harm will come to the environment, and it is completely risk-free to operate.

## 1.6 Reactor types utilized for the oxidative desulfurization of gas oil

### 1.6.1 Trickle Bed Reactors (TBR)

Trickle bed reactors hold significant relevance within the three-phase (gas-liquid-solid) reaction systems found in industrial applications. In a petroleum refinery, these processes are employed for hydrotreating, oxidation, hydrodesulfurization, and hydrocracking. Typically, TBRs operate within a pressure range of (20–30) bar. This range is essential for minimizing catalyst deactivation, enhancing the solubility of gaseous reactants, boosting conversion rates, and optimizing heat transfer (Azarpour et al., 2021). The primary disadvantage is the complexity of gas-liquid flow over porous catalyst particles in

TBRs. Liquids may exhibit varying degrees of wetting on surfaces (Nigam & Larachi, 2005).

TBRs have been employed in published ODS research (Gheni et al., 2017), which explored the continuous ODS of 2-propyl Mercaptan and n-butyl Mercaptan using a cobalt-supported activated carbon catalyst (2% Co/AC) and molecular oxygen as an oxidant. The reaction was investigated under various conditions, including temperatures ranging from 100 to 400°C, liquid hour space velocities (LHSV) between 2.5 and 10 $h^{-1}$, and initial concentrations of 2-propyl Mercaptan and n-butyl Mercaptan, both set between 75 and 300 ppm. The study revealed that 2-propyl Mercaptan exhibits higher reactivity compared to n-butyl Mercaptan. Additionally, the oxidation process was found to have no significant impact on the physical properties of naphtha. Under the investigated operating conditions, the oxidation rate was observed to increase with temperature and decrease with LHSV.

TBR was used to conduct the ODS process at moderate oxidation temperatures, aiming to evaluate the effectiveness of the synthesized catalysts for a continuous three-phase ODS process. The evaluation research on ODS considered various factors, including temperatures of 60 and 70 °C, LHSVs of 1, 1.35, 2, and 4 $h^{-1}$, pressures of 6 and 800 kPa, and initial sulfur concentrations of 100 and 300 ppm. The removal efficiency of n-butyl Mercaptan during processing in the TBR was notably high for both coated and uncoated catalysts. Optimal performance was achieved at a temperature of 70 °C, a pressure of 800 kPa, a liquid hourly space velocity of 1 $h^{-1}$, and an initial sulfur concentration of 300 ppm (H. R. Mohammed et al., 2022).

### 1.6.2 Batch Reactors

A batch reactor represents the most fundamental form of reactor vessel utilized in chemical or industrial processes. A standard batch reactor consists of a tank where chemical reactions occur. Moreover, these tanks are equipped with an agitator and feature an internal heating or cooling system. Throughout the reaction, there is no addition or removal of reactants from the reactor; it can operate with either a homogeneous or heterogeneous reaction mixture. A common drawback of the batch reactor is the labor required to empty and fill the tank between operations. Recent advancements in computer control have eliminated this disadvantage. The

interval between batches has become the primary drawback of batch reaction processes (Foutch & Johannes, 2003). The oxidation process of sulfur compounds was conducted using a batch reactor. A three-necked round-bottom flask is utilized for ODS reactions. The central neck is linked to a vertical condenser that effectively condenses the light gas oil vapor while permitting only air to escape. In the second cuff, the flask will serve as an air source for the compressor, with air traveling to the bottom of the flask via the glass tube. The temperature within the flask can be accurately measured by inserting a thermometer into the third neck. and to extract a sample of the product from inside the flask. The heating process results in the batch reactor being heated and combined with a magnetized stirrer (Ali et al., 2009).

A number of investigations utilizing batch reactors for ODS have been documented in the literature.

(Jarullah et al., 2020) conducted an investigation into the elimination of the sulfur compound ethyl mercaptan found in light naphtha feedstock ODS using a batch reactor. A homemade Nanocatalyst (ZnO/zeolite nanoparticles) was utilized alongside air as the oxidant, exploring various reaction conditions such as temperatures, times, and initial sulfur concentrations. The highest experimental conversion of sulfur compounds achieved with this method reached 90.5% using a handcrafted nanocatalyst consisting of 8% ZnO/zeolite nanoparticles. Considering the specified operating conditions (temperature = 323 K, batch time = 40 min, and initial concentration = 250 ppm).

(Jose et al., 2011) The oxidation of thiophene was carried out in a batch method using $H_2O_2$ as the oxidizing agent and Cu/TS-1 as the catalyst. Evidence suggests that copper on TS-1 greatly improves conversion rates. The best values for the three process variables were reaction temperature at 70 °C, catalyst weight at 0.45 g, and hydrogen peroxide per mole of thiophene at 19.9 mol. This led to a 93% conversion rate. An activation energy of 28.67 kJ/mol was determined for the Cu/TS-1 catalyst.

### 1.6.3 Oscillatory Baffled Reactor (OBR)

OBR is a tubular reactor characterized by sharp-edged orifice baffles that are evenly distributed along its length, as illustrated in Figure 1.9 This reactor features a periodic oscillatory (or pulsed) flow that is superimposed on a net flow. The oscillatory flow is generated through the motion of the piston and diaphragm

located at the bottom of the reactor. The pulsed flow engages with the baffles, generating vortices that induce fluctuations in the laminar flow, leading to enhanced transverse movements and optimized transport efficiency (Avila et al., 2022).

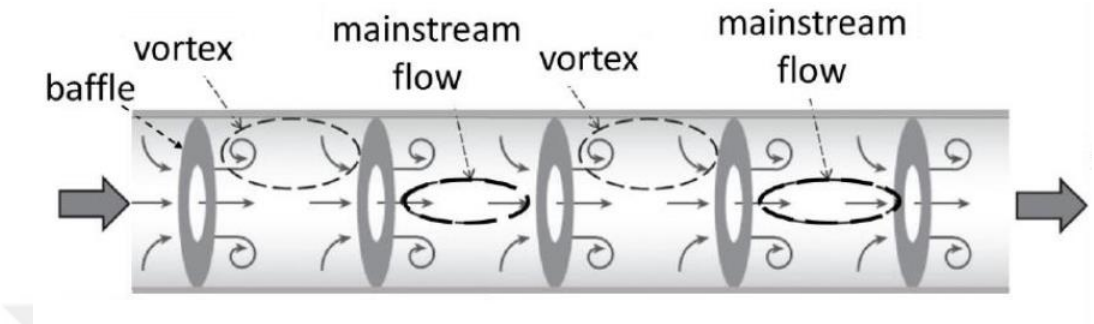


**Figure 1.9.** illustration of fluid dynamics within an Oscillatory Baffled Reactor (Laybourn et al., 2019)

Various baffle geometries are available; each designed to serve specific purposes such as minimizing frictional losses or enhancing mixing. Options include integral, central axial, helical, and wire wool baffles, as illustrated in Figure 1.10. These geometries aim to enhance the adaptability of the screening platform owing to their "plug and play" characteristics. Every baffle design serves a distinct function. The smooth constrictions of the "integral baffle" design prove to be especially advantageous for applications sensitive to shear, including bioprocesses. They have also been utilized for gas-liquid suspension and solids suspension.

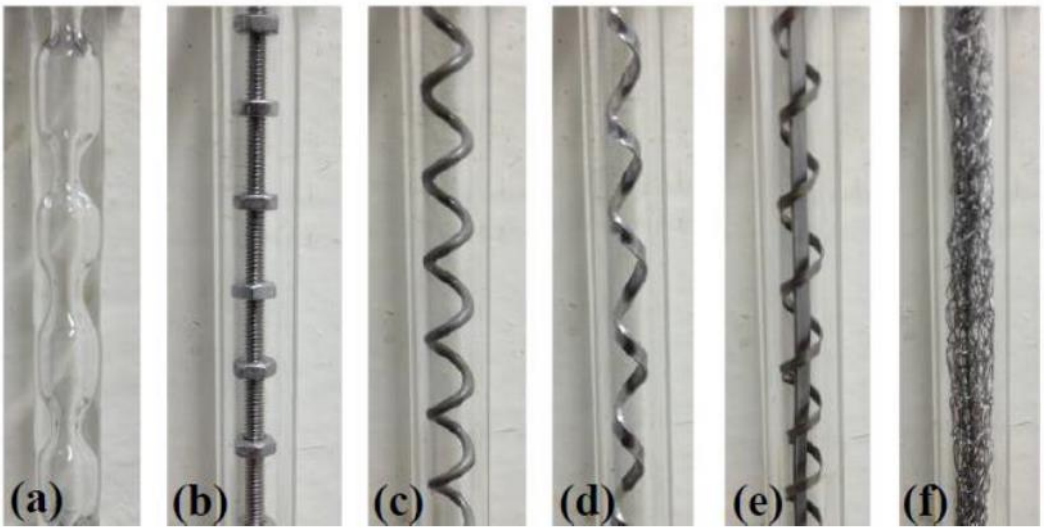


**Figure 1.10.** Baffle configurations; (a) integral baffles, (b) central axial baffles, (c) round-edged helical baffles, (d) sharp-edged helical baffles, (e) sharp-edged helical baffles with a central insert, (f) wire wool baffles (McDonough et al., 2015a)

Helical baffles including a central insert and wire wool configurations enhance the inter-phase dispersion of immiscible liquids. The central axial design is preferred for homogeneous liquid reactions because it offers greater shear compared to the integral design. The helically baffled design offers advantages for solid-liquid reactions due to its less constricted main flow, which leads to reduced particle blockage. This design offers enhanced operational flexibility compared to alternative systems, as it can achieve a significant level of plug flow across a broad spectrum of oscillation conditions (Phan et al., 2011a, 2012).

The fluid dynamics of the OBR reactors are influenced by the geometric parameters which are detailed in Table 1.4.

**Table 1.4.** The dimensionless groups and dynamic parameters used in the oscillatory flow (Abbott et al., 2013a)

| Parameter | Symbol | Equation | Description |
|---|---|---|---|
| baffle spacing | L | - | The shape and length of vortex |
| Baffle Spacing Ratio | $n_b$ | $\frac{l_b}{D}$ | Influences eddy expansion |
| Baffle Open Area | $S$ | $(\frac{d_o}{D})^2$ | Controls eddy width |
| frequency of oscillation (Hz) | $f$ | - | Number of oscillations per second |
| Volumetric flow rate (ml/ min) | $Q$ | - | The volume of material entering the OBR over a given time |

Within these parameters, ($L_{b)}$ represents the baffle spacing, (D) denotes the inner diameter of the OBR, ($d_O$) indicates the baffle constriction diameter, ($\rho$) refers to the fluid density, $u$ signifies the superficial fluid velocity, (μ) stands for the fluid viscosity, $(f)$ corresponds to the oscillation frequency, and ($X_o$) describes the oscillation amplitude (center-to-peak). Figure 1.11 illustrates these parameters.

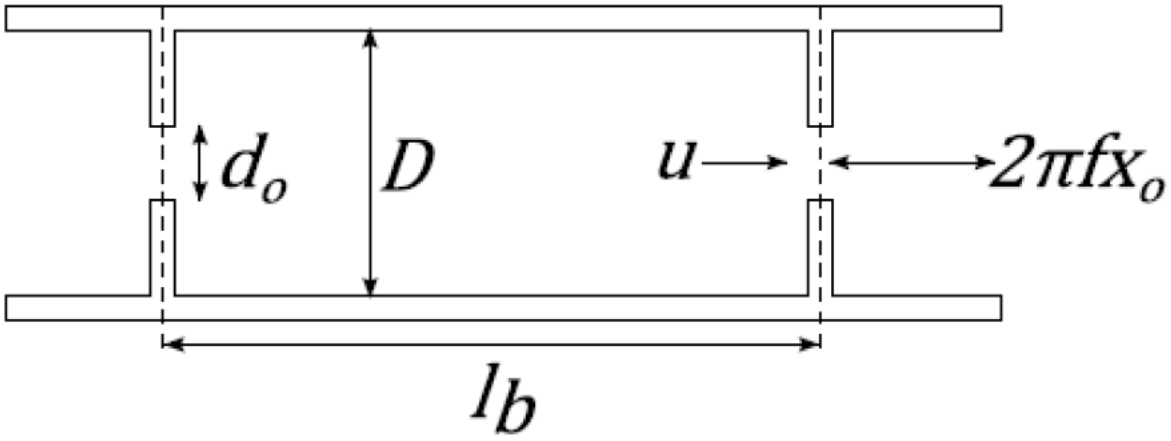


**Figure 1.11.** Oscillatory motion across a geometric parameter and net flow diagram(Abbott et al., 2013a)

### 1.6.4 The advantages from (OBR)

OBRs offer several advantages over traditional CSTRs and tubular reactors:

1. **Versatility:** OBRs can operate in both batch and continuous modes, and in both horizontal and vertical orientations (McDonough et al., 2015a).
2. **Compact Design:** OBRs can achieve extended space times under plug flow conditions, allowing for more compact reactor designs (Phan et al., 2012).
3. **Enhanced Mixing:** The vortex cycle in OBRs ensures uniform radial mixing, reducing heat and concentration gradients. This leads to shorter reaction times and more consistent mixing patterns throughout the reactor (McDonough et al., 2015a).
4. **Flexible Mixing:** OBRs offer a wide range of mixing conditions, from soft mixing characteristic of plug flow to more intense mixing approaching mixed flow conditions. This flexibility allows for precise control over mixing intensity and residence time distribution (RTD) (McDonough et al., 2015a).
5. **Improved Solid Suspension:** OBRs effectively suspend and convey solids in the radial direction, making them suitable for processes involving solid particles (McDonough et al., 2015a).
6. **Gentle Mixing:** OBRs exhibit lower and more uniform shear compared to STRs, making them ideal for shear-sensitive organisms and large molecules (Abbott et al., 2013a, 2013b; X.-W. Ni, 2006).

7. **Scalability:** OBRs can be scaled up linearly by maintaining specific dimensionless numbers (St, Reo, Ren), allowing for reliable prediction of mixing intensity and flow conditions in larger reactors based on laboratory-scale experiments (Jian & Ni, 2005).
8. **Enhanced Heat Transfer:** OBRs with oscillatory components exhibit increased heat transfer compared to non-oscillatory reactors, leading to improved thermal performance (Anderson et al., 2009).
9. **Improved Mass Transfer:** OBRs promote better mass transfer due to uniform bubble size and higher gas holdup, leading to increased reaction rates and efficiency (Anderson et al., 2009).

## 1.7 Heterogeneous catalysts applied in oxidative desulfurization (ODS)

Heterogeneous catalytic systems utilized in oxidation reactions. The ease of separating products and catalysts is a notable advantage of heterogeneous systems. Similar to findings in homogeneous ODS systems, heterogeneous catalysts have predominantly been employed to model feedstock and hydro treated middle distillate fractions containing low sulfur levels, with the ODS reaction serving as a finishing process. Heterogeneous catalysts primarily consist of a single active phase, typically derived from transition metals, which is dispersed on a support exhibiting a high specific surface area (Houda et al., 2018). Active metals exhibit instability and readily lose their catalytic activity due to their sensitivity to external conditions (Argyle & Bartholomew, 2015). Among the diverse catalysts employed in ODS, such as ODS catalysts supported on zeolite (Wang, Jibrin, et al., 2020), ODS catalysts supported on $SiO_2$ (Piva et al., 2021), ODS catalysts Supported on $\gamma$-$Al_2O_3$ (Beshkoofeh et al., 2021), ODS catalysts supported on H-ZSM-5 (Sharifi et al., 2019), ODS catalysts supported on Graphene Oxide (Otaghsaraei et al., 2022), ODS catalysts supported on activated carbon (A. E. Mohammed et al., 2024).

### 1.7.1 ODS catalysts supported on zeolite

Zeolite is a solid substance characterized by a distinct microporous architecture, uniform acidic and basic sites, and notable thermal and hydrothermal

stability (Wang, Wang, et al., 2020). Metal nanoparticles supported on zeolites have been utilized in various important industrial processes, such as hydrogenation, cracking, and catalytic isomerization (Primo & Garcia, 2014). In these instances, the majority of metal nanoparticles are deposited onto the surfaces of zeolite crystals. There are several opportunities for the development and production of more effective catalysts due to the zeolites' use in containing and protecting active structures and in selecting reactants, products, or transition states (Čejka et al., 2012; Choi et al., 2010; Thomas et al., 2005). Crystalline microporous materials allow molecules to preferentially access intracrystalline active sites according to their size or shape due to the small and homogenous size of their channels and gaps (Moliner et al., 2015; Pérez-Ramírez et al., 2008). Small clusters are typically stabilized more efficiently against sintering and poisoning in confined environments compared to less constrained mesoporous structures. Numerous studies have investigated metal oxides supported on zeolite in the context of oxidative desulphurization.

(Dadashi et al., 2020) synthesized Mo/HY catalysts containing varying amounts of Mo (3, 5, 10, 20 wt.%) using the impregnation method and evaluated their performance in the oxidative desulfurization of dibenzothiophene (DBT) in model oil. HY zeolite was utilized in this study because of its appropriate textural characteristics, including a three-dimensional large pore diameter that enhances mass transfer and shape selectivity. The catalyst samples were characterized using XRF, XRPD, FT-IR, UV-vis, $N_2$ adsorption-desorption, SEM-EDX, TEM, and NH3-TPD analyses. Increasing the molybdenum content to 20 wt.% led to a reduction in mesopore volume and a decrease in the strength of the acidic sites. Conversely, polymeric non-framework Mo was generated on the catalyst surface as the Mo content increased to 20 wt.%. The catalyst with 3 wt.% of Mo exhibits optimal activity, attributed to the presence of isolated framework Mo species. Approximately 100% of sulfur was eliminated from the model oil containing 1000 ppm DBT utilizing Mo (3 wt.%)/HY under specified mild conditions (O/S = 2, T = 60 °C, Mcatalyst/Voil = 8 g/L, 90 min, VSolvent/VOil = 1/2). The removal of DBT achieved 90% following three cycles of recycling. The hydrophilicity of HY resulted in the catalyst being adversely affected by the aqueous phase containing acetonitrile.

(Dadashi et al., 2020) employed a wet impregnation method to prepare a series of HPW/MWW catalysts, subsequently utilizing them in the oxidative desulfurization of model oil and real gasoline oil, with $H_2O_2$ used as the oxidant and MeCN as the extractant. Findings indicate that the catalyst HPW/MWW-40 shown significant catalytic activity at dosage of 0.03 g, a temperature of 60 °C, initial S concentrations of 500 mg/L, O/S ratios of 4:1, and oil to catalyst ratios of 1:2. The elimination rate of DBT reached 99.8% under optimal reaction conditions. Following three cycles, HPW/MWW-40 was effectively regenerated through ethanol washing. The catalyst was utilized on straight-run gasoline and FCC gasoline sourced from (Maoming Petrochemical) Company. The high olefin content in FCC gasoline resulted in a sulfur removal rate of only 46.9%, whereas straight-run gasoline achieved a removal rate of 98.1%.

## 1.8 Preparation of Catalysts Using Incipient Wetness Impregnation (IWI)

One popular method of manufacturing heterogeneous catalysts is incipient wetness impregnation (IWI), which is easy to understand and implement. In order to wetting the particles and fill the pores, the active metal feedstock are often dissolved in a large enough volume of solvent, such as water or an organic solution. There are two main ways in which precursors can be dissolved during impregnation: "dry impregnation" (DI) occurs when the volume of solution does not exceed the pore space, and "wet impregnation" (WI) occurs when an excessive amount of an aqueous or organic solution is used to dissolve the active metal precursor. Incipient wetness impregnation (IWI) necessitates the assessment of the support's pore volume immediately before synthesis, aligning this measurement with a precise volume of the precursor solution to achieve a more uniform distribution. Impregnation occurs during the diffusion process when the solution exceeds the pore volume of the support. The diffusion of solute into the pores occurs as a result of the concentration gradient of the active component. The removal of pore moisture and air from the support was achieved through heating or evacuation to enhance the diffusion of the solute into the support's pores during the impregnation step. This step may occasionally be deemed unnecessary. Figure 1.12 illustrates the sequence of steps (Richardson, 2013).

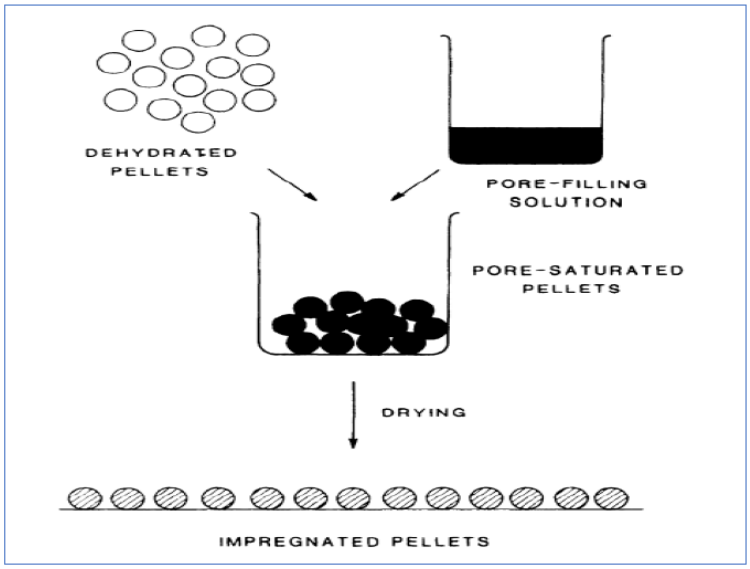


**Figure 1.12.** Procedures for the Impregnation of the Active Component (Richardson, 2013)

Drying the sample is essential for the removal of the solvent through gradual heating until the boiling point of the solvent is attained. The elimination of the solvent from the pores results in enhanced crystallization of the salt on the pore surfaces. Uniform salt deposition takes place when the rate of crystallization is sufficiently slow (Tengco, 2016). The calcination of the sample, alongside the drying step, is essential for preparing the active catalyst. Calcination is a thermal processing method employed to transform salt into an oxide or mineral. It also eliminates bound or crystallized water from catalysts (Mehrabadi et al., 2017).

(Y. Liu et al., 2019) synthesized $SnO_2/Al_2O_3$ composite oxide catalysts with varying $SnO_2$ content using an impregnation method. $SnCl_2{\cdot}2H_2O$ was dissolved in ethylene glycol to create a stable solution. The $\gamma$-$Al_2O_3$ support was impregnated with this solution and stirred for an hour. (Piao et al., 2021) Prepared (WOx/meso-$SnO_2$) catalysts with different WOx loadings (10-30 wt.%) using incipient wetness impregnation. (NH4)$6H_2W_{12}O_{40}{\cdot}xH_2O$ solution was impregnated onto meso-$SnO_2$ support, dried overnight at 80 °C, and then calcined at 400 °C for 3 hours in static air. (Otaghsaraei et al., 2022) synthesized $SnO_2$/rGO catalysts with varying tin oxide loadings (5-20 wt.%) using incipient wetness impregnation. $SnCl_2{\cdot}2H_2O$ was dissolved in methanol, and the solution was added to dried GO. The mixture was

dried at 65 °C for 12 hours and then calcined at 350 °C for 5 hours under an argon atmosphere.

## 1.9 Aims and Objectives of This Study

The primary goal of this research is to develop a catalytic desulfurization process that leverages an efficient and selective oxidative desulfurization (ODS) process. This involves employing a heterogeneous catalyst and hydrogen peroxide ($H_2O_2$) as an oxidant to achieve ultra-deep desulfurization of Iraqi gas oil cut fuel while minimizing energy consumption and environmental impact.

To accomplish this, the study will focus on the following specific objectives:

1. **Reactor Design and Implementation:**

- Design and scale-up of a batch and continuous OBR using a helical baffle design.
- Installation of the reactor to simulate real-world operational conditions.

2. **Catalyst Preparation:**

- Synthesis of a Pd/Zeolite catalyst using the Incipient Wetness Impregnation (IWI) method.

3. **Performance Evaluation:**

- Investigation of the impact of various operating conditions on the desulfurization efficiency of light gas oil.

4. **Optimization:**

- Determination of optimal process settings for the oxidative desulfurization process.

# 2. MATERIALS and METHOD

## 2.1 Introduction

This chapter examines the preparation and characterization of catalyst for the oxidative desulfurization (ODS) process, as well as the installation, design, and operation of an oscillatory baffled reactor (OBR). The apparatus employed to facilitate, obtain, and analyze the experimental data for sulfur removal from (light gas oil) cut through the ODS process in a two phase (solid-liquid) batch mode OBR unit, employing a nano-catalyst made of (Pd/Zeolite) and an oxidizing agent such as hydrogen peroxide ($H_2O_2$) under varied working conditions. The experimental work consists of the following steps:

1. Preparation of the catalyst utilizing the incipient wetness impregnation (IWI) method, homemade palladium on zeolite (Pd/Zeolite) Nano-catalyst.
2. Characterization of the synthesized catalyst utilizing advanced surface science methodologies.
3. Evaluate the catalytic performance of the prepared catalyst for the oxidative desulfurization (ODS) in a batch mode oscillatory baffled reactor (OBR) across a wide range of operating conditions:
    - Reaction temperature (40, 60, and 80℃).
    - Reaction time (4, 8, and 12 min).
    - Oscillation frequency (0.4, 0.8 and 1.2 Hz).
4. Analyzing the effect of operating conditions on sulfur conversion and identifying optimal conditions for maximum sulfur removal efficiency.

## 2.2 Materials

### 2.2.1 Feedstock

This study utilized light gas oil as the feedstock, sourced from the Refineries Company in Iraq. The feedstock specifications are presented in Table 2.1.

**Table 2.1.** Specifications of light gas oil

| Physical property | Physical values |
|---|---|
| Flash point, (℃) | 67 |
| Specific gravity@15.5℃ | 0.8433 |
| Total sulfur, (ppm) | 624 |
| API at 60F | 38.33 |
| Kinematic viscosity at 40℃ (mm2 /sec) | 3.22 |
| Initial boiling point (℃ ) | 162 |
| Final boiling point (℃ ) | 362 |

### 2.2.2 Oxidant

Hydrogen peroxide ($H_2O_2$) is used as an oxidizing agent; the specifications are detailed in Table 2.2.

**Table 2.2.** Specifications of Hydrogen peroxide ($H_2O_2$)

| **Specification** | **Physical values & Supplier** |
|---|---|
| Chemical Formula | $H_2O_2$ |
| State (Solid-liquid) | Liquid |
| Melting Point ℃ | - 0.43 |
| Boiling Point ℃ | 150.2 |
| Molecular Weight (g/mol) | 34 |
| Purity wt.% | 30 |
| Manufacturer/Provider | Sigma-Aldrich, Germany |

### 2.2.3 Catalysts

#### 3.2.3.1 Support

The synthesized catalyst was supported by a commercially available beta nano zeolite powder. Table 2.3. displays the beta-zeolite parameters.

**Table 2.3.** Beta-zeolite nano powder parameters

| **Parameter** | **Physical values & Supplier** |
|---|---|
| Appearance | White powder |
| Pore volume | ≥ 0.16 $cm^3$/gm |
| SSA | < 180 $m^2$/gm |
| $SiO_2$ content | ~ 6% |
| $Al_2O_3$ content | ~ 48% |
| Particle size | ≥ 100 nm |
| Manufacturer/Provider | XFNANO Materials Tech Co., Ltd - China |

#### 3.2.3.2. Active component

In this study, we identified palladium (Pd) as the active component of the catalyst. The precursor utilized was palladium chloride salt ($PdCl_2$). The specifications for palladium chloride are presented in Table 2.4.

**Table 2.4.** Specifications of palladium (II) chloride

| **Parameter** | **Physical values & Supplier** |
|---|---|
| Chemical structure | $PdCl_2$ |
| Appearance (Form) | Powder |
| Purity % | 99.9% |
| Solubility (Color) | Brown to Dark |
| Molecular weight (g/mol) | 177.33 |
| Melting point °C | 678-680 |
| Manufacturer/Provider | Sigma-Aldrich, Germany |

## 2.3 Preparation of Catalyst

The zeolite was loaded with Pd using the Incipient Wetness Impregnation (IWI) technique (Nawaf et al., 2019). Figure 2.1 represent the steps involved in catalyst preparation, following is a description of the steps:

1. Dissolving of 0.638 gm of ($PdCl_2$) in 30 ml of Distilled water using a magnetic stirring for an hour until the salt dissolves completely.

2. 6 gm of (Zeolite) add gradually to the solution prepared in step one with continues mixing for 3 hours, to guarantee the homogeneity between (salt and support).
3. Transfer the mixture to the Ultrasonic sonicator, medium process (Power set at 40% with 0.1 pulses for duration of 80 minutes), the sample was left to rest for 7 hours.
4. Evaporate the mixture using a magnetic stirring hot plate at 80 °C.
5. The impregnated (Pd/zeolite) catalyst underwent drying in an electric oven at 80◦C overnight to remove water content from the surface and pores, as well as to crystallize the salt on the pore surface.
6. Finally, the dry sample was calcinated in the furnace at specified temperatures of (150 ℃ for 1 hour, 250 ℃ for 1 hour, 400 ℃ for 1.5 hours, and 550 ℃ for 2.5 hours), with an oxygen flow rate to enhance the conversion of the metal salt to metal oxides.
7. The sample stayed in the oven overnight to allow for gradual cooling to gain the Pd/Zeolite catalyst.

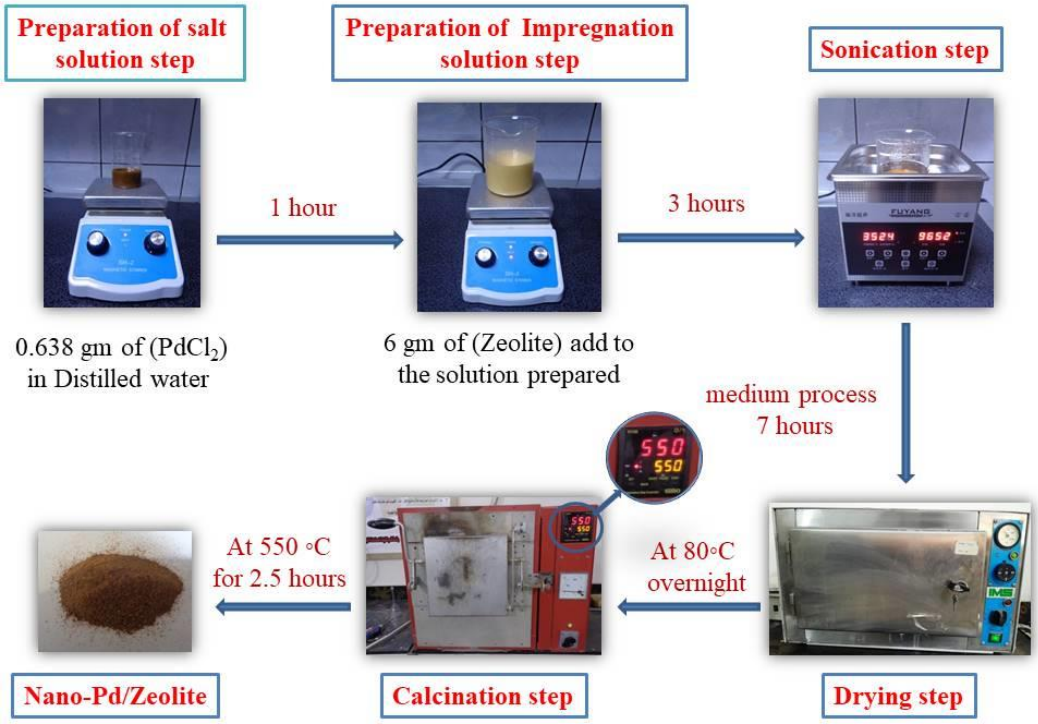


**Figure 2.1.** The steps involved in catalyst preparation

## 2.4 Characterization of the catalyst

### 2.4.1 FT-IR analysis

FT-IR spectroscopy is commonly utilized to identify functional groups in catalyst materials. FT-IR analysis was conducted in the Geology Department at the College of Science, University of Tikrit, using the FTIR-8400S instrument from Shimadzu, Japan. Figure 2.2 illustrates the setup.

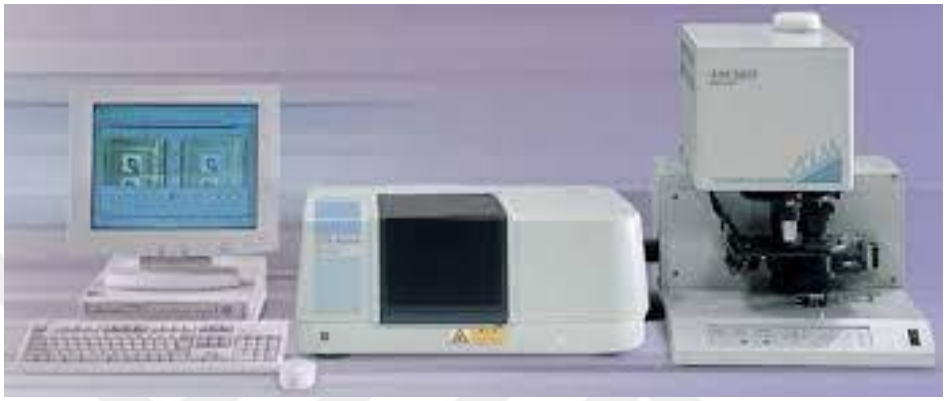

**Figure 2.2.** FT-IR system setup

### 2.4.2 BET (N2 Adsorption/Desorption)

The specific surface area (SBET), and pore properties, and average diameter of the catalyst (Pd/Zeolite) were determineding use the $N_2$ Adsorption/Desorption. The test was done at the University of Tehran, Iran, utilizing the Brunauer Emmett and Teller (BET) method as per ISO-9277-2010 standards. Figure 2.3 illustrates the setup.

**Figure 2.3.** Surface area analysis system

0.1658 g of catalyst powder was measured and positioned within a sample cell assembly. The physisorption gas utilized was molecular nitrogen, with a cross-sectional area of 0.162 nm² for the nitrogen molecule. The isotherms of adsorption and desorption utilized in BET surface area analysis were acquired at the boiling point of liquid nitrogen (77 K).

### 2.4.3 FESEM- EDX analysis

The Field Emission Scanning Electron Microscope (FESEM) is an electron microscope that generates images of a sample by scanning it with a focused electron beam. Electrons interact with atoms in the sample, generating signals that provide information regarding the sample's surface topography and composition. Characteristic X-rays generated from the interaction of electrons with the sample can be detected in a scanning electron microscope (SEM) that is equipped for energy-dispersive X-ray spectroscopy (EDX). The analysis of X-ray signals facilitates the identification of composition and quantification of elemental abundance in the sample. The surfice morphology and distribution of chemical elements in Pd/Zeolite catalysts were analyzed using a device equipped with energy-dispersive X-ray spectroscopy (EDX), wavelength-dispersive X-ray spectroscopy (WDX), a secondary electron (SE) detector, a backscatter electron detector (BSD), and electron backscatter diffraction (EBSD). The focus distance was set at 6.11 mm, with a magnification range from 100x to 30,000x during the analysis. FESEM-EDX tests were performed by using MIRA3 device at the University of Tehran, Iran. Figure 2.4 illustrates the FESEM-EDX instrument.

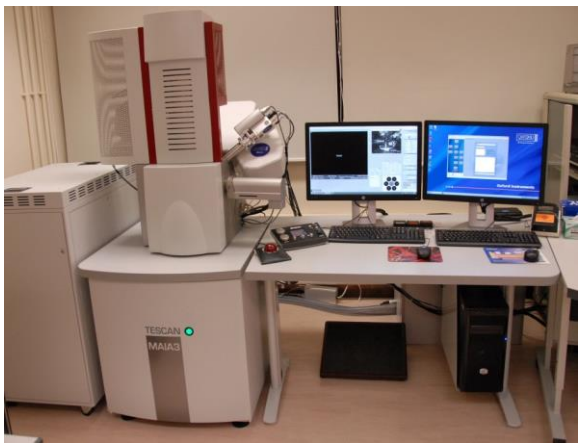


**Figure 2.4.** MIRA3 Electron Microscope

### 2.4.4 XRD (X-Ray Diffraction) analysis

X-Ray diffraction analysis (XRD) is a nondestructive method that yields detailed data relating to the crystallographic structure, chemical composition, and physical properties of materials. This study utilized X-ray diffraction (XRD) to identify the phases in the catalyst, employing a PANalytical X'Pert PRO MPD diffractometer with Cu Kα radiation (λ = 1.54 Å), an electron current of 30 mA, and an accelerating voltage of 40 kV. The operational range for XRD was 2θ from 10° to 80°, with a scanning speed of 3 degrees per minute. Phases were identified through comparison with reference data from the Joint Committee on Powder Diffraction Standards (JCPDS) data files. XRD tests were performed at the University of Tehran, Iran. Figure 2.5 illustrates the XRD instrument.


**Figure 2.5.** The XRD device setup

### 2.4.5 TGA (Thermogravimetric Analysis)

Thermogravimetric analysis is a method that quantifies the mass of a material over time or temperature, subjecting the sample to a regulated temperature protocol within a controlled setting. A thermogravimetric analyzer (TGA) comprises a sample pan that is mounted on a precision balance. The pan is located in a furnace and is subjected to heating or cooling throughout the experiment. The sample's mass is monitored throughout the experiment. A sample purge gas regulates the sample environment. The gas may be classified as either inert or reactive, flowing over the sample or exiting via an exhaust system. The TGA tests

were performed at the University of Tehran in Iran. The analysis protocol involved heating the sample from 25 to 1001 ℃ at a rate of 20 ℃/min in a nitrogen atmosphere. Figure 2.6 illustrates the TGA instrument.

**Figure 2.6.** The TGA instrument

## 2.5 Experimental setup

The pilot plant of the OBR unit was designed for batch sulfur oxidation for evaluating the performance of Pd/Zeolite catalysts in the ODS process for Iraqi light gas oil cut. This unit's main section is the reactor. The structure consists of a cylindrical tube that is surrounded by an effective heat source (heater) and is thermally insulated using a high-performance insulator. The feedstock (light gas oil), was contained within a feed tank. The feedstocks and catalyst were introduced from a storage tank via the catalyst slot via a pump. The fluid's oscillatory motion through the reactor was controlled by a variable-stroke piston pump. The oxidant, hydrogen peroxide ($H_2O_2$), was delivered through a dosing pump linked to an appropriate storage container. Figures 2.7 and 2.8 present a schematic diagram of the unit alongside an image of the setup. The OBR experimental apparatus is composed of several components:

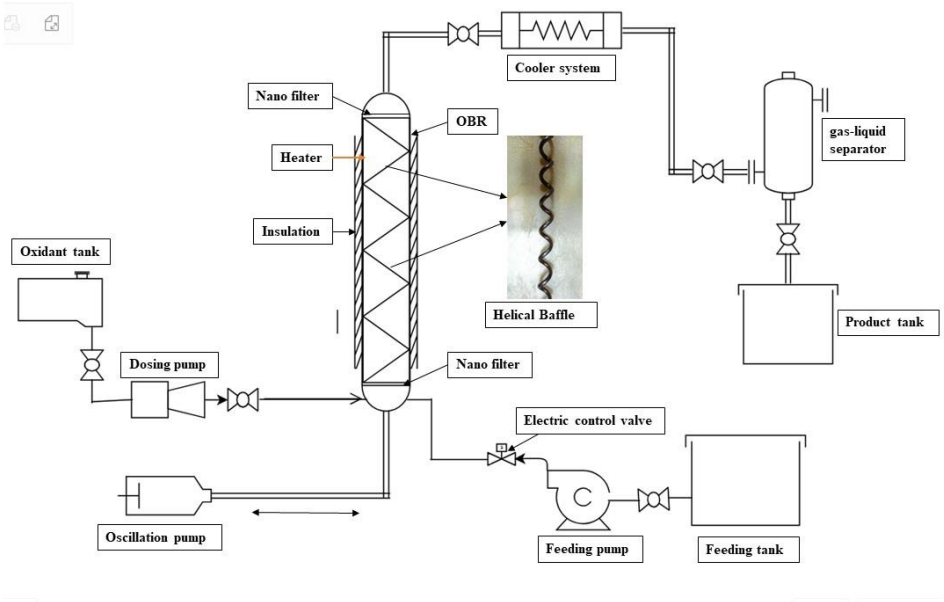


**Figure 2.7.** Schematic diagram of OBR unit

**Figure 2.8.** Experimental setup of the OBR unit

### 2.5.1 The reactor design

The pilot plant reactor was constructed using molybdenum-bearing austenitic stainless steel (SS-316). The reactor's dimensions and insulation details are provided in Table 2.5 It has three inlet ports: two for the feedstock and oxidant,

and one for the oscillation process. The product exits through a single outlet slot. Clean diesel samples were collected from the outlet port after each oxidation period. The reactor, equipped with a heater, can maintain temperatures between 0 and 150 °C. A temperature controller ensures precise temperature control. The reactor was fabricated in a workshop in Baghdad, Iraq. A specific set of dimensionless groups was used to standardize the reactor's operation.

**Table 2.5.** Reactor design and construction specs

| No. | Parameter | Value |
|---|---|---|
| **1.** | Inside diameter (mm) | 16 |
| **2.** | Height of reactor (mm) | 600 |
| **3.** | Volume of reactor (ml) | 120 |
| **4.** | thickness of the tube (mm) | 1 |
| **5.** | Flung diameter (mm) | 90 |
| **6.** | The insulation (mm) | length 600, thickness 25 |

### 2.5.2 Design a Helical Baffle inside the Reactor

Selection and design of the helical baffle type for the pilot plant were established, ensuring that the helical baffle reactor (OBR) was oriented vertically

and secured to an oscillation system to facilitate the oscillation of the light gas oil. The helical design significantly improves mass and heat transfer during the ODS process. The chosen baffle geometries were selected to ensure optimal mixing (X. Ni et al., 1998). The baffle was produced in a private workshop located in Baghdad's Industrial District, Iraq, utilizing high specifications and stainless steel (SS-316). The ratio of the wire diameter to the tube diameter was (one). The ratio between the helical pitch and the tube diameter was consistent with the baffle spacing observed in traditional OBR (Phan & Harvey, 2012). The geometrical characteristics of the helical baffle are presented in Table 2.6 Figure 2.9 is an illustrative image of the designed helical baffle.

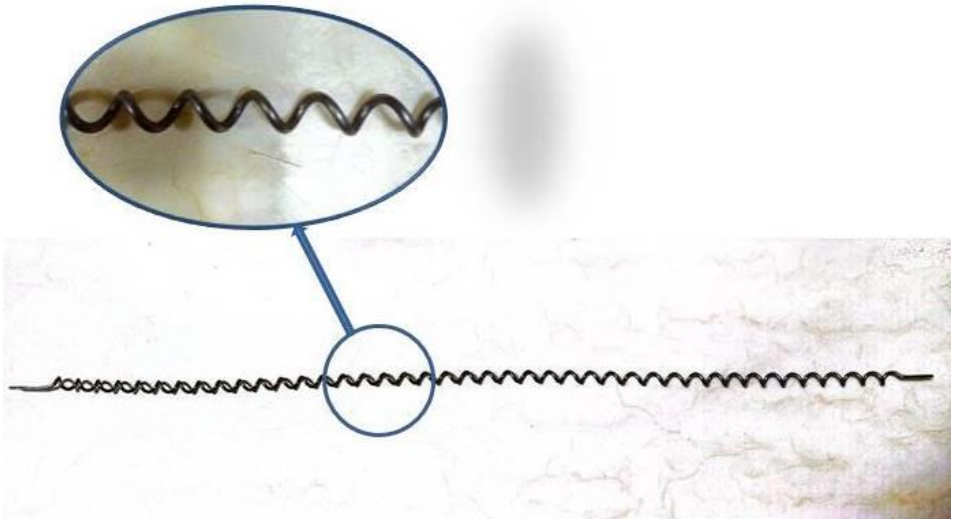

**Figure 2.9.** Design of the helical baffle

**Table 2.6.** The geometrical characteristics of the helical baffle

| No. | Parameter | Value |
|---|---|---|
| **1.** | Diameter of helical baffle (mm) | 12 |
| **2.** | Thickness of the baffle wire (δ) (mm) | 1.7 |
| **3.** | Helical baffle spacing ( $l$ ) (mm) | 22.5 |
| **4.** | Length of Helical (L) (mm) | 590 |

### 2.5.3 Oscillatory pump

A new design of an oscillatory pump that generates oscillations (frequency) in the OBR unit has been introduced. The pump consists of a cylindrical plunger made from high-grade stainless steel (SS-316), as detailed in Table 2.7 The motor changes its displacement via a connected shaft. The oscillatory pump generates frequency motion within the tubular reactor, resulting in fluid oscillation inside the reactor. The oscillatory pump varies the oscillation frequency within the range of f = 0.01–150 Hz. This study regulated frequency oscillation based on the motor's speed via a frequency controller device, with voltage ranging from 0 to 30 volts.

**Table 2.7.** Specification of oscillation pump

| **Parameter** | **Value & Supplier** |
|---|---|
| Plunger diameter (cm) | 5 |
| Plunger length (cm) | 10 |
| Shaft length (cm) | 15 |
| Motor power supply (V) | DC (0-30) |
| Motor Manufacture | Japan |

### 2.5.4 Feeding pump

The tubular reactor was connected via a stainless-steel tube with a commercial pump. The pump was used to supply feedstock (light gas oil) from a

storage tank to the OBR. The amount of fuel supplied to the reactor is controlled by the pump using a flow rate control device. The pump specifications are presented in Table 2.8.

**Table 2.8.** Specification of Feeding pump

| **Parameter** | **Value** |
|---|---|
| Working voltage | DC24V |
| Medium | Liquid |
| Flow Rate | 830 ml/min |
| Max. Pressure | 160 psi |
| Max. Hydraulic Head | 2.5 m |
| Working environment temperature | 0 – 40 ℃ |

### 2.5.5 Oxidant pump

The tubular reactor was linked through a stainless-steel tube to a dosing pump (DP).The pump facilitated the transfer of a specific volume of the oxidant (hydrogen peroxide) from the storage tank to the OBR. The specifications of the pump are detailed in Table 2.9 The function of the dosing pump (DP) is to deliver a precise quantity of the oxidant ($H_2O_2$) in the process accurately and at controlled intervals. The amount of oxidant was controlled via the dosing pump using an electrical voltage regulator.

**Table 2.9.** Specification of dosing pump

| Parameter | Value |
|---|---|
| Working voltage | DC 12V |
| Medium | Liquid |
| Flow Rate | 1-30 ml/min |
| Max. Static Suction Lift | 2m $H_2O$ |
| Max. Hydraulic Head | 2m $H_2O$ |
| Working environment temperature | 0 – 40 ℃ |

### 2.5.6 Controlling of the operational parameters of the unit

The controllers act as auxiliary parts for effective control of the OBR unit. The reactor's temperature was regulated using an advanced industrial temperature controller (Diy More, Ltd.; China). This instrument is a multifunctional microprocessor-controlled device. The main Specification of the temperature controller that was used in this study are shown in Table 2.10.

**Table 2.10.** Specification of temperature controller

| Specification | Value |
|---|---|
| Supply voltage | DC 12-72V |
| Temperature range | -40℃ - 120℃ |
| Measurement accuracy | 0.1 ℃ |
| Working environment temperature | -20℃ - +70℃ |
| Display | LCD |

The amount of feedstock entering the reactor was controlled using an advanced industrial flow rate control system (DI JIANG, ZJ-LCD-M, China). The main specification of the flow system controller that was used in this study are shown in Table 2.11.

**Table 2.11.** Specification of flow rate control system

| Specification | Value |
|---|---|
| Flow Rate | 0.5-30 L/min |
| Working voltage | DC 4.5-15V |
| Suffering Pressure | Max 1.5Mpa |
| Accuracy | ± 0.5% |
| Working temperature | -20℃ - +80℃ |
| Display | LCD |

The oscillation pump speed is controlled using an advanced industrial frequency control system (FY1002S DDS, FY Electronics China). This system regulates the voltage supplied to the pump by adjusting the frequency. The main specification of the frequency system controller that was used in this study is shown in Table 2.12.

**Table 2.12.** Specification of oscillation pump control system

| Specification | Value |
|---|---|
| Working voltage | DC 0.5 - 30 V |
| Frequency range | 0.01 Hz – 2 MHz |
| Frequency Resolution | 0.01 Hz – (10 mHz) |
| Frequency Stability | $\pm 1\times10^{-6}$ |
| Frequency Accuracy | $\pm 5\times10^{-6}$ |
| Display | LCD |

### 2.5.7 The storage system

The pilot reactor plant is equipped with a storage system that includes a feed tank designated for the feedstock (light gas oil), which is transferred to the reactor unit through a pump. Additionally, there is an oxidant container for the oxidant agent ($H_2O_2$), which is introduced into the reactor via a dosing pump. Finally, a

product storage tank is utilized for the collection of the output generated by the reactor.

## 2.6 Experimental procedure

### 2.6.1 Unit preparation

Before the experiment could begin, the OBR unit was prepared according to the following protocol:

1. Installation and connection of the helical baffle within the reactor.
2. Operation of the control system responsible for controlling the reaction conditions.
3. The OHBR unit underwent cleaning prior to each experiment to guarantee safety in the work conducted. Ethanol is used as an appropriate solvent. It is capable of removing any material from the pilot plant prior to operation.
4. The system was checked for leaks using $N_2$ gas at a pressure of 2 bar, maintained for 30 minutes to review the safety of the system.
5. The operating conditions of the OBR unit were evaluated. The reactor was loaded with feedstock, and the trial run was conducted at the maximum designed operating conditions (frequency 1.2 Hz and temperature 80 ℃) for one hour shortly before operation.

### 2.6.2 Plan of the experimental work (Operating Conditions)

This study involved conducting various experiments at an experimental scale under the following moderate operating conditions:

- Type of catalyst: Nano - Pd/Zeolite.
- Reaction temperature (40, 60, and 80 ℃).
- Reaction time (4, 8, and 12 min).
- Oscillation frequency (0.4, 0.8 and 1.2 Hz).

### 2.6.3 Running of experiments

The complete factorial run planned for the evaluation of the nano-Pd/Zeolite catalyst in the OBR is listed in Table 2.13 It is important to dry the prepared catalyst, Pd/Zeolite, in an oven for 3 hours at 120 ℃ just before its application in the unit.

**Table 2.13.** Design of the full factorial runs

| RUN | Temperature (ºC) | Frequency (Hz) | Time (min) |
|---|---|---|---|
| 1 | 40 | 0.4 | 4 |
| 2 | 60 | 0.4 | 4 |
| 3 | 80 | 0.4 | 4 |
| 4 | 40 | 0.4 | 8 |
| 5 | 60 | 0.4 | 8 |
| 6 | 80 | 0.4 | 8 |
| 7 | 40 | 0.4 | 12 |
| 8 | 60 | 0.4 | 12 |
| 9 | 80 | 0.4 | 12 |
| 10 | 40 | 0.8 | 4 |
| 11 | 60 | 0.8 | 4 |
| 12 | 80 | 0.8 | 4 |
| 13 | 40 | 0.8 | 8 |
| 14 | 60 | 0.8 | 8 |
| 15 | 80 | 0.8 | 8 |
| 16 | 40 | 0.8 | 12 |
| 17 | 60 | 0.8 | 12 |
| 18 | 80 | 0.8 | 12 |
| 19 | 40 | 1.2 | 4 |
| 20 | 60 | 1.2 | 4 |
| 21 | 80 | 1.2 | 4 |
| 22 | 40 | 1.2 | 8 |
| 23 | 60 | 1.2 | 8 |
| 24 | 80 | 1.2 | 8 |
| 25 | 40 | 1.2 | 12 |
| 26 | 60 | 1.2 | 12 |
| 27 | 80 | 1.2 | 12 |

## 2.7 Analysis of products

The residual sulfur content of the desulfurized light gas oil samples was analyzed. The X-ray sulfur analyzer represented in Figure 2.10 was utilized at the Baiji refinery in Iraq. according to D7039 G3, ASTM D7039, and ISO 20884 standards.


**Figure 2.10.** The X-Ray sulfur analyzer

# 3. RESULTS

## 3.1 FTIR Spectroscopy results

The design of the prepared catalyst utilizing zeolite as a support and active compounds (Pd/zeolite) was examined through FTIR analysis. Reference spectra for zeolite were acquired to comprehensively understand the impact of active compounds on the catalyst. Figure 3.1 illustrates the FTIR analysis within the wave number range of 4000 to 400 $cm^{-1}$.

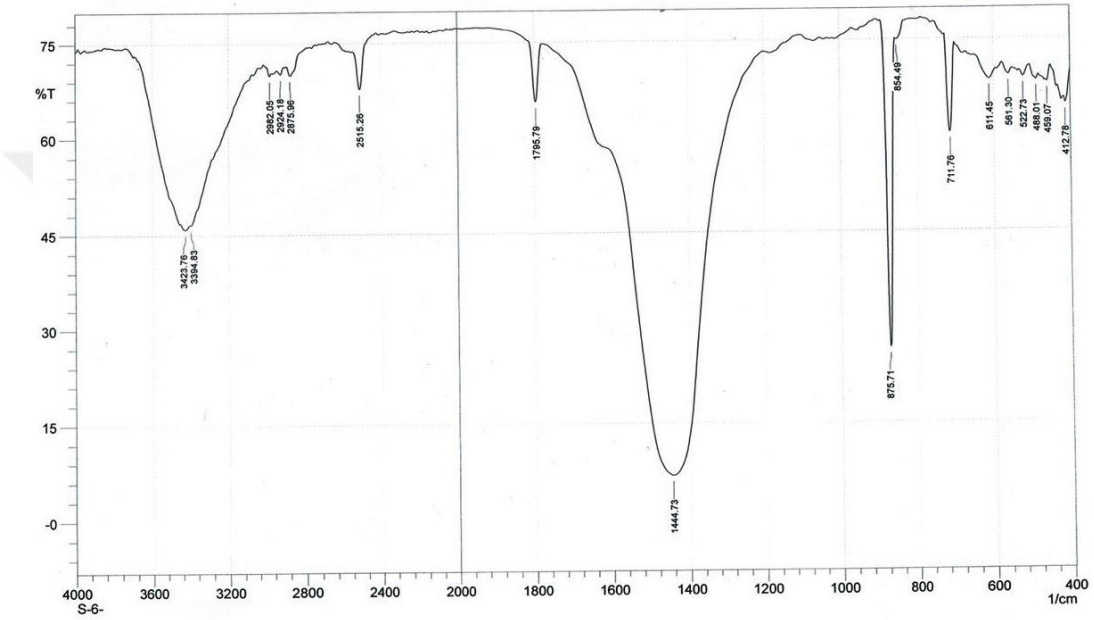


**Figure 3.1.** FTIR Spectroscopy of (Pd/zeolite) catalyst

## 3.2 XRD results

X-ray diffraction (XRD) was used to analyze the crystal structure of the Pd/zeolite catalyst as shown in Figure 3.2.

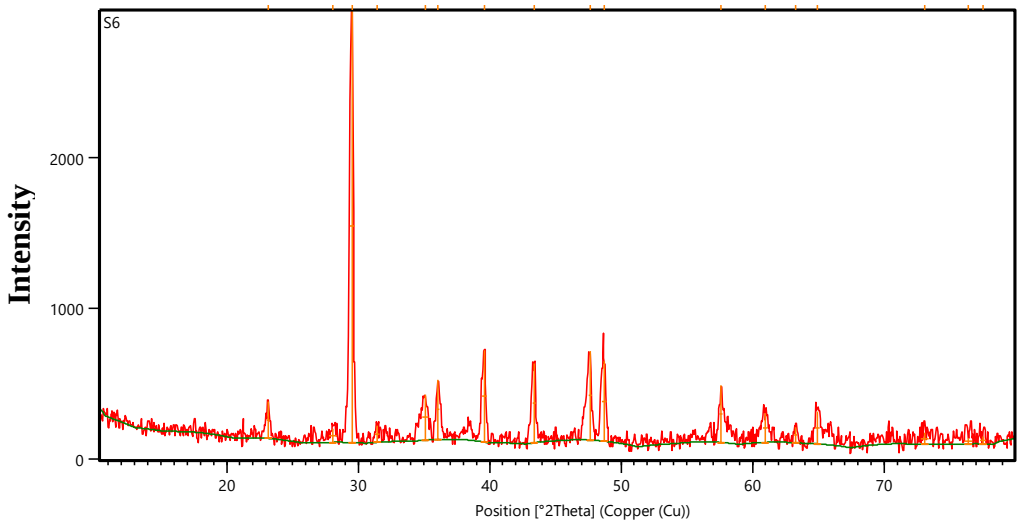


**Figure 3.2.** XRD profiles for catalyst prepared Pd/zeolite

### 3.3 FESEM-EDX results

The surface morphology of the synthesized catalyst was analyzed through FESEM images at varying magnifications, and energy dispersive X-ray (EDX) techniques. The FESEM results are in Figure 3.3 presented distribution of the zeolite particles.

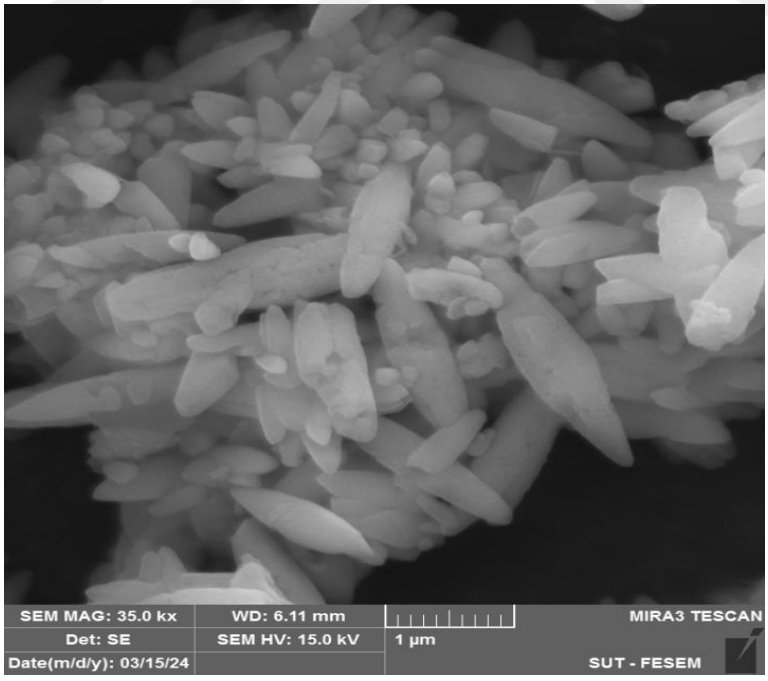


**Figure 3.3.** FESEM Images of Zeolite

Figure 3.4 illustrates the surface structure acquired through FESEM analysis of the Pd/zeolite catalyst.

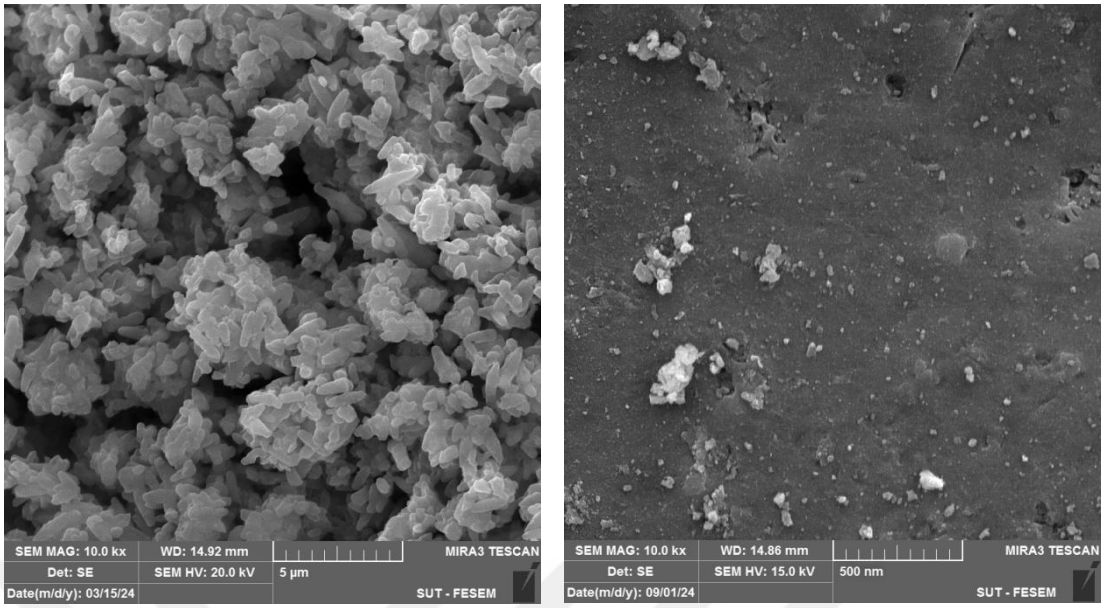


**Figure 3.4.** FESEM Images of Pd/Zeolite catalyst

The energy dispersive X-ray (EDX) analysis was performed following the loading of the active metal onto the zeolite to assess the catalyst's surface composition. The spectrum obtained from EDX, as illustrated in Figure 3.5, indicates the presence of surface elements: 46.19 wt. % oxygen (O), 43.64 wt. % aluminum (Al), 3.32 wt. % silicon (Si), and 6.85 wt. % palladium (Pd).

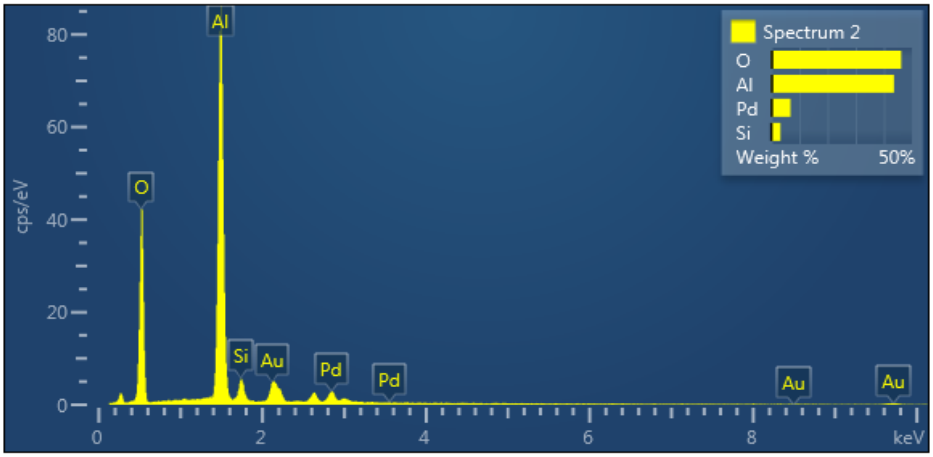


**Figure 3.5.** EDX map spectrum for the Pd/Zeolite catalyst

Figure 3.6 presents the EDX map utilized to analyze the elemental distribution within the Pd/zeolite catalyst through the measurement of Kα line intensity across the sample.

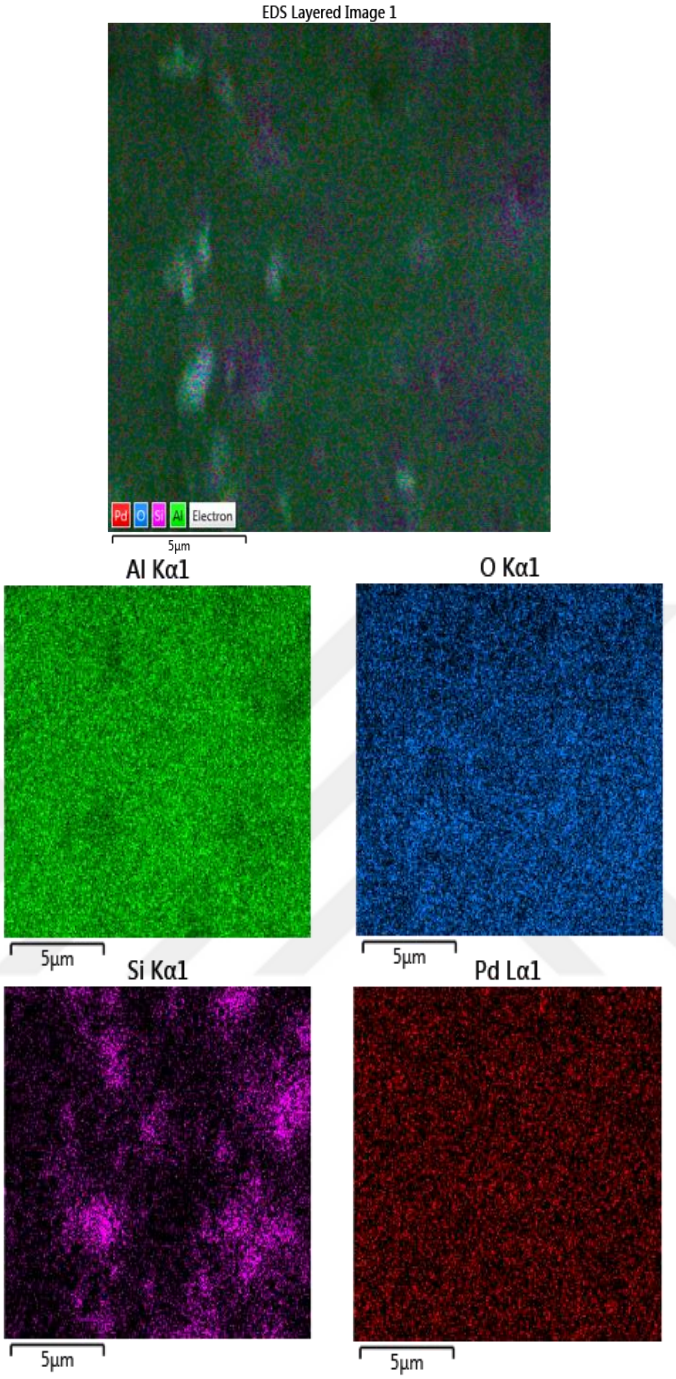


**Figure 3.6.** EDX Kα maps of element distribution of Pd/zeolite catalyst

### 3.4 Surface area and pore size results

Surface BET was used to calculate the specific surface area and average pore diameter ($D_{average}$). for evaluating a total volume, $N_2$ gas was utilized. The surface area of the materials (Zeolite and Pd/Zeolite) was computed using the $N_2$-(ADS) / (DES) isotherm data at a relative pressure ($P/P_o$) as seen in Figures 3.7 and 3.8 To determine the volume of all materials, the amount of $N_2$ gas adsorbed at a

(P/Po) of 0.99 is converted to the corresponding liquid volume of the adsorbate ($N_2$). The $N_2$ gas was utilized to calculate the Langmuir surface area of the materials (Zeolite and Pd/Zeolite) at 77 °K with a 12-hour degassing period, As indicated in Table 3.1.

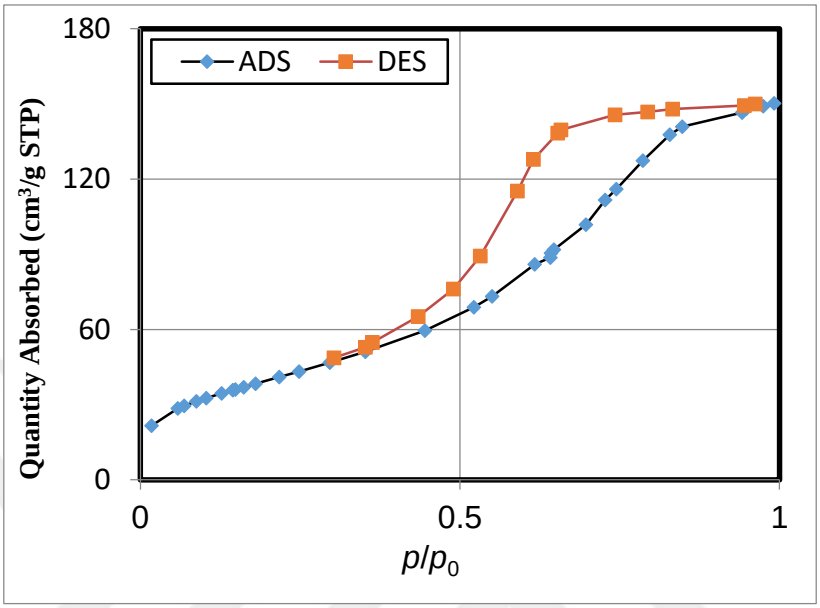


**Figure 3.7.** $N_2$-adsorption-desorption isotherm for Zeolite support

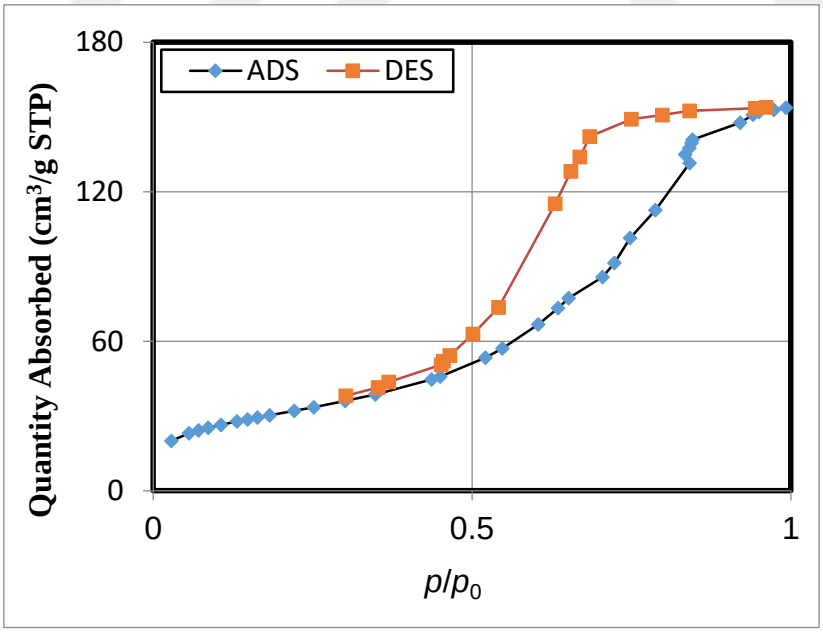


**Figure 3.8.** $N_2$-adsorption-desorption isotherm for Pd/Zeolite catalyst

**Table 3.1.** Surface area and pore volume information of the catalyst

| Sample | as, BET ($m^2 g^{-1}$) | as, Lang ($m^2 g^{-1}$) | Total pore volume($p/p_0$=0.99) ($cm^3 g^{-1}$) | $D_{ave}$ (nm) |
|---|---|---|---|---|
| Zeolite | 149.31 | 145.99 | 0.2377 | 8.3938 |
| Pd/Zeolite | 113.26 | 122.79 | 0.198 | 6.2208 |

### 3.5 Thermogravimetric analysis (TGA) results for (Pd/ zeolite) catalyst

The (TGA) analysis determines the variation in weight of (Pd/zeolite) samples examined across a temperature range of 0–1000 ℃. The catalyst (Pd/zeolite) examined in this study underwent evaluation for thermal stability through the test.

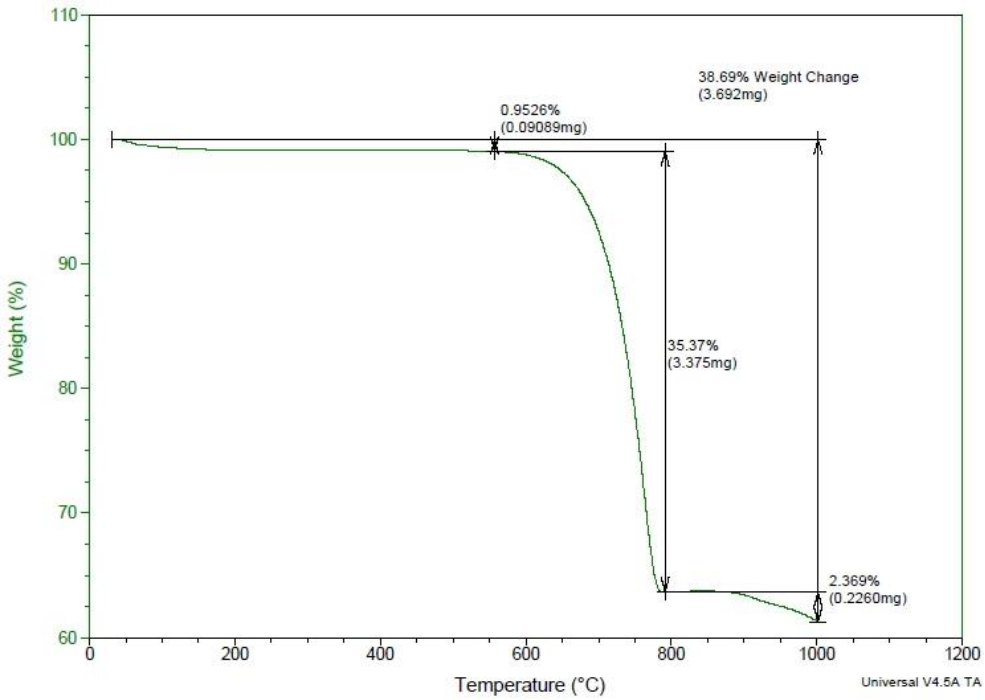


**Figure 3.9.** TGA curves for Pd/zeolite

## 3.6 Optimization of the ODS process in OBR design as a function of operational conditions

### 3.6.1 Samples Analysis

The desulfurization efficiency in the ODS process of the OBR is illustrated in the Table 3.2, for more details of the calculation was used shown in appendex 2.

**Table 3.2.** The results of the full factorial runs after X-Ray sulfur analyzer

| NO. | Temperature (°C) | Frequency (Hz) | Time (min) | Initial con. (ppm) | Result (ppm) | Conversion (%) |
|---|---|---|---|---|---|---|
| 1 | 40 | 0.4 | 4 | 624 | 345 | 44.71 |
| 2 | 60 | 0.4 | 4 | 624 | 200 | 67.95 |
| 3 | 80 | 0.4 | 4 | 624 | 196 | 68.59 |
| 4 | 40 | 0.4 | 8 | 624 | 269 | 56.89 |
| 5 | 60 | 0.4 | 8 | 624 | 109 | 82.53 |
| 6 | 80 | 0.4 | 8 | 624 | 98 | 84.29 |
| 7 | 40 | 0.4 | 12 | 624 | 259 | 58.49 |
| 8 | 60 | 0.4 | 12 | 624 | 102 | 83.65 |
| 9 | 80 | 0.4 | 12 | 624 | 87 | 86.06 |
| 10 | 40 | 0.8 | 4 | 624 | 260 | 58.33 |
| 11 | 60 | 0.8 | 4 | 624 | 176 | 71.79 |
| 12 | 80 | 0.8 | 4 | 624 | 162 | 74.04 |
| 13 | 40 | 0.8 | 8 | 624 | 166 | 73.40 |
| 14 | 60 | 0.8 | 8 | 624 | 80 | 87.18 |
| 15 | 80 | 0.8 | 8 | 624 | 62 | 90.06 |
| 16 | 40 | 0.8 | 12 | 624 | 161 | 74.20 |
| 17 | 60 | 0.8 | 12 | 624 | 69 | 88.94 |
| 18 | 80 | 0.8 | 12 | 624 | 54 | 91.35 |
| 19 | 40 | 1.2 | 4 | 624 | 214 | 65.71 |
| 20 | 60 | 1.2 | 4 | 624 | 160 | 74.36 |
| 21 | 80 | 1.2 | 4 | 624 | 146 | 76.60 |
| 22 | 40 | 1.2 | 8 | 624 | 114 | 81.73 |
| 23 | 60 | 1.2 | 8 | 624 | 69 | 88.94 |
| 24 | 80 | 1.2 | 8 | 624 | 50 | 91.99 |
| 25 | 40 | 1.2 | 12 | 624 | 103 | 83.49 |
| 26 | 60 | 1.2 | 12 | 624 | 55 | 91.19 |
| 27 | 80 | 1.2 | 12 | 624 | 43 | 93.11 |

# 4. DISCUSSION

## 4.1 Introduction

This chapter presents and analyzes the results of catalyst characterization and the evaluation of the prepared Pd/zeolite catalyst for the oxidative desulfurization of light gas oil in an OBR. The discussion will also explore the influence of operational parameters, including temperature, oscillatory frequency, and residence time, on the conversion process.

## 4.2 Catalyst characterization

### 4.2.1 FTIR Spectroscopy

As illustrates in Figure 3.1, no alterations in the positions of characteristic absorption peaks were observed for the catalyst, and all peaks aligned with zeolite characteristics. The FTIR spectra of the as-dried synthesized catalyst exhibit a broad band in the range of 3000–3800 $cm^{-1}$ and 1300–1800 $cm^{-1}$, corresponding to the bound hydroxyl groups and isolated OH groups, which are attributed to the stretching and bending modes of adsorbed water (Choeichom & Sirivat, 2018; Xie et al., 2023). This suggests a significant level of acidity on the surface of the prepared catalyst, enhancing the interaction between the surface and various organic compounds, including sulfur atoms.

The primary distinctive peaks of the zeolite were observed between 600 and 1200 $cm^{-1,}$ corresponding to the vibrations of Al-O and Si-O. The various bonds observed, particularly at a wavenumber of approximately 850–950 $cm^{-1}$, correspond to symmetric Si-O stretching. A minor peak around 1000–1200 $cm^{-1}$ is linked to asymmetric Si-O stretching, while the band between 650–800 $cm^{-1}$ corresponds with Al-O bending vibrations. This suggests the presence of different coordinated Al species in zeolite (Xie et al., 2023). Additional peaks within the range of 458 to 651 $cm^{-1}$ correspond with the vibration of the Pd-O bending (G. Abbas et al., 2019). The results show that Pd has been effectively grafted onto the zeolite surface and remains present in the functionalized material following calcination at 550 ˚C.

### 4.2.2 XRD results

The XRD pattern Figure 3.2 revealed distinct peaks at 39.6°, 47°, and 68.3°, corresponding to the (111), (200), and (220) planes of face-centered cubic (FCC)

Pd, respectively. According to the standard references (JCPDS card 05-0681) and (JCPDF 46-1043). the intense and broadened peaks indicate the formation of well-crystallized, small Pd nanoparticles.

The XRD pattern Figure 3.2 also showed characteristic peaks at 22.9°, 28.08°, and 29.52°, corresponding to the zeolite structure. This suggests that the impregnation process did not significantly alter the zeolite's structure. The negatively charged zeolite surface acted as adsorption sites for positively charged $Pd^{2+}$ ions, leading to the formation of PdO particles. The XRD results indicate a high dispersion of palladium oxide on the zeolite support.

### 4.2.3 FESEM-EDX results

The FESEM results presented in Figure 3.3 validated the diverse size distribution of the zeolite particles, indicating that the particles exhibit a broad spectrum of sizes and shapes, along with a more porous morphology. This observation highlights the benefits of a high surface area due to elevated porosity, which leads to effective adsorption capacity for active compounds like palladium oxide.

As shown in Figure 3.4, an outstanding distribution of palladium oxide particles over the support zeolite surface was observed. The white areas indicate the presence of palladium, whereas the dark semi-white areas denote the zeolite surface. Furthermore, Figure 3.4 illustrates that an acceptable active particle size distribution was attained due to the extensive sonication applied to both the active material and the support. The sonication process effectively inhibited the agglomeration of active metal on the surface, thereby improving the metal's dispersion. This indicates that the sonication procedure serves as a particularly efficient technique for generating active metal (palladium oxide) on zeolite dispersed catalysts in comparison to alternative preparation methods. The presence of porosity and cavities in these materials leads to a heightened adsorption capacity, enabling them to adsorb elevated concentrations of sulfur effectively.

As illustrated in Figure 3.5, the elevated percentage of oxygen in the catalyst can be attributed to the substantial oxygen content in silica and alumina, the primary constituents of the zeolite. The presence of a palladium peak was observed in the

Pd/zeolite catalyst at 6.85 wt. %, which corresponds to the intended quantity established during the catalyst's preparation using the IWI method.

The figure Figure 3.6 displayed the distribution of O, Si, Al, and Pd. The distribution of palladium on zeolite appears to be well-structured; aligning with the findings presented in the FESEM images Figure 3.3 additionally, the findings from the structural analysis showed that the loading of active material would not lead to considerable damage to the pores and morphology of the catalyst. These materials can be utilized as highly efficient adsorbents and are applicable in various industrial and environmental contexts.

### 4.2.4 Surface area and pore size

The provided data (Figures 3.7, 3.8 and Table 3.1) indicates that the Zeolite support has a BET-specific surface area of 149.13 $m^2/g$ and a mesopore volume of 0.2377 $cm^3/g$, suggesting good adsorbent properties. The support has an average pore radius of 83.938 Å (or 8.3938 nm), which falls within the mesopores category (2-50 nm). After catalyst preparation, the specific surface area, pore volume, and average pore size decreased. The BET surface area of the support reduced to 113.26 $m^2/g$. This reduction is attributed to the blockage of micropores and tunnels in the zeolite by the palladium composite during calcination. Despite the reduction in surface area, the catalyst maintained a high mesopore content, increasing the number of active sites. This enhancement facilitated better adsorption and improved the oxidation desulfurization reaction rate.

### 4.2.5 Thermogravimetric analysis (TGA) for (Pd/ zeolite) catalyst

For the TGA analysis, this reaction removes residual oxygen from Al-O and Si-O when the oxygen levels exceed the necessary amount in the structure or when dealing with unstable metal oxides (Zhang et al., 2020). The TGA curve of the synthesized catalyst (Pd/zeolite) indicates that material decomposition happened in three distinct regions, as illustrated in Fig. 4.9 A minimal weight loss of 0.0474 % occurred due to moisture removal during the heating of the catalysts from the first moment of heating to approximately 113.54 °C. This loss results from the moisture that vaporization in the sample. Subsequently, it was observed that the mass remains stable as the temperature increases until it reaches 562.17 °C. The sample weight decreased from 99.04% to 63.67 % in the second region. In the third region,

the weight loss of approximately 0.226 mg, representing 2.369%, reflects the loss attributed to the de-oxygenation reaction, which involves the removal of excess oxygen from the Si-O and Al-O structures.

The observed total mass loss values in the TGA experiments for the (Pd/Zeolite) are approximately 38.69 %. The highest rate of weight loss occurred within the temperature range of 562.17 to 782 °C, indicating the significant thermal stability of the synthesized Pd/zeolite. The data indicate that the weight of catalysts varies with increasing temperature as a result of thermal treatment. The observed change, specifically weight loss, is attributed to the release of various compounds, including adsorbed moisture, volatile compounds, and the decomposition of $PdCl_2$ into metal oxide, as indicated by the curve (Kim & Chung, 2003).

The results indicated that the prepared Pd/zeolite catalyst shows good thermal stability and significant advantages in the ODS process. The catalyst demonstrates optimal thermal stability.

## 4.3 Optimization of the ODS process in OBR design as a function of operational conditions

### 4.3.1 Impact of Reaction Time on OBR Sulfur Removal

This study examined how reaction time (τ), affects sulfur removal from light gas oil through an oxidation reaction. The investigation was conducted at various time intervals of 4, 8, and 12 minutes, maintaining a constant reaction temperature, oscillation frequency, and atmospheric pressure at 1 atm. A composite catalyst (Pd/Zeolite) weighing 0.15 gm and 2 ml of hydrogen peroxide ($H_2O_2$) were utilized as the oxidant in the ODS process. This manuscript presents measurements of the total sulfur content (instead of the sulfur species or compounds), focusing on the values obtained both before and following the oxidative desulfurization process.

The experimental results show that increasing the residence time in the oscillatory baffle reactor significantly improves sulfur removal. For example, at 1 atm, 0.4 Hz, and 40 °C, increasing the residence time from 4 to 8 minutes led to a sulfur removal increase from 44.71% to 56.89 % Figure 4.10a. Similarly, at 0.8 Hz and 60 °C, increasing the residence time from 4 to 8 minutes resulted in a sulfur conversion increase from 71.79 % to 87.18 % Figure 4.10b. These improvements are attributed to the increased contact time between reactants and the mesoporous

Pd/Zeolite catalyst, facilitating better diffusion of sulfur and oxygen atoms within the catalyst's pores. However, further increasing the residence time beyond 8 minutes led to diminishing returns, likely due to the accumulation of water byproducts and reduced interaction between reactants and the catalyst Figure 4.10a, 4.10b, and 4.10c.

Extending the residence time of oxidation reduces flow fluctuations, allowing for better interaction between sulfur compounds and hydrogen peroxide ($H_2O_2$) at the active sites, leading to the formation of sulfoxide and sulfone (Phan et al., 2011b). Longer contact times between $H_2O_2$ molecules and sulfur within the porous structure enhance the oxidation reaction.An optimal residence time of 12 minutes was found to achieve a removal efficiency of 93.11%.

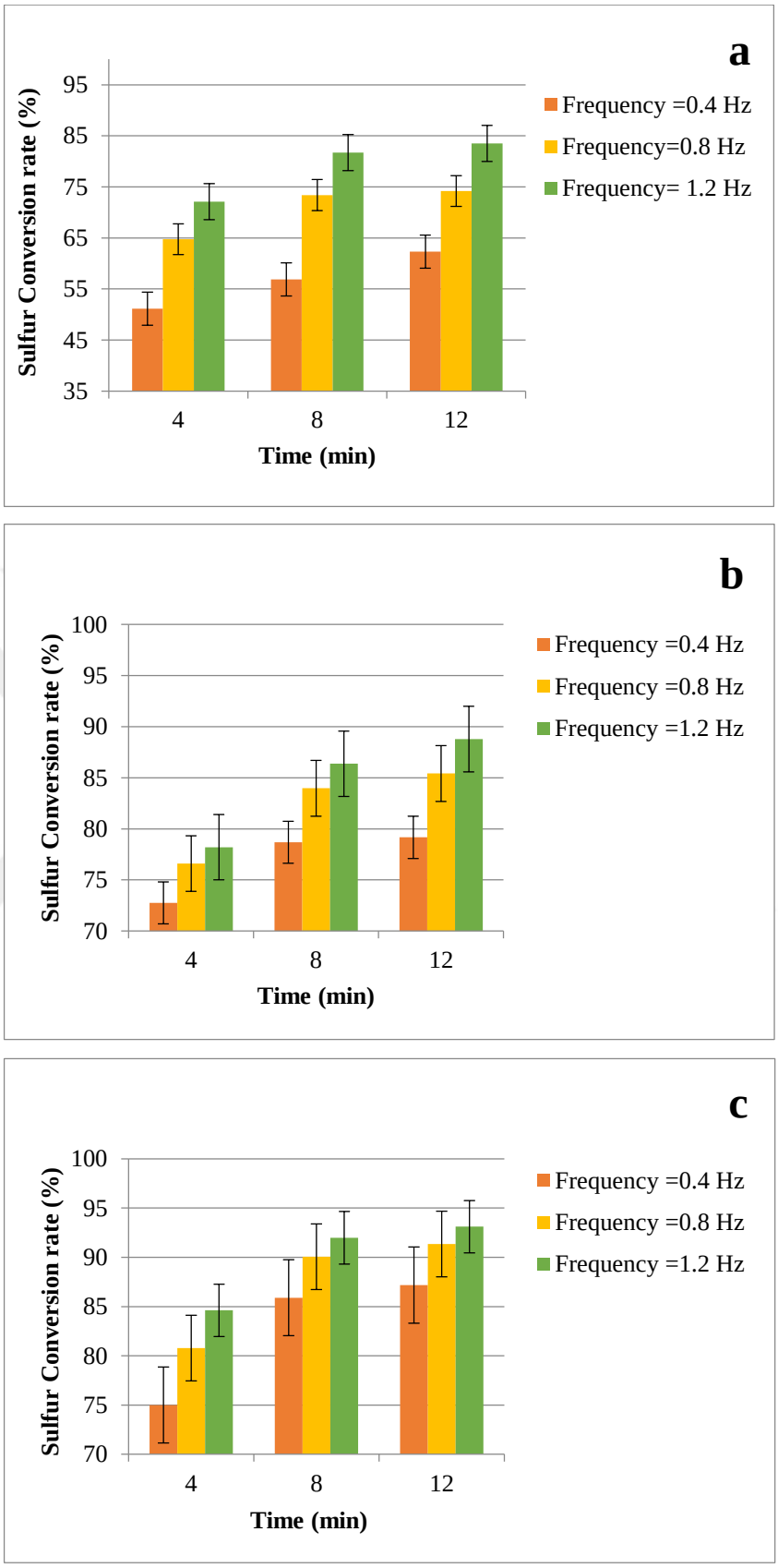


**Figure 4.1.** Impact of reaction time on sulfur removal using (Pd/Zeolite) at: (a) T = 40°C, (b) T = 60°C, (c) T = 80°C.

### 4.3.2 Impact of Reaction Temperature on OBR Sulfur Removal

To investigate the effect of temperature on the oxidative desulfurization process, a series of experiments were conducted at 40, 60, and 80 °C, while keeping residence time and oscillation frequency constant. Hydrogen peroxide (2 ml) and 0.15 g of Pd/Zeolite catalyst were used at 1 atm. These results showed that increasing of temperature from 40 to 80 °C improved sulfur removal efficiency.

Figure 4.11a shows that increasing the temperature from 40 to 60 °C at a frequency of 0.4 Hz and a residence time of 4 minutes improved sulfur removal from 44.71% to 67.95%. Further increasing the temperature to 80 °C led to a sulfur conversion of 68.59%.Figure 4.11b gives that at a frequency of 0.8 Hz and a residence time of 8 minutes, increasing the temperature from 40 to 60 °C improved sulfur removal from 73.4% to 87.18%. At 80 °C, the sulfur conversion reached 90.06%. Figure 4.11c also illustrates that at a residence time of 12 minutes and a frequency of 1.2 Hz, increasing the temperature from 60 to 80 °C improved sulfur conversion from 91.19% to 93.11%.

The experimental findings demonstrated that an increase in oxidation temperature to 80 ˚C led to a reduction in sulfur content, therefore resulting in a conversion rate that reached an optimal 93.11 %, as reported by (Hameed et al., 2023a). ODS shows a significant temperature dependence.

Increasing the oxidation temperature reduces fuel viscosity and surface tension while increasing diffusivity. These changes enhance the transport rate between reactants, leading to a faster reaction rate. Consequently, raising the oxidation temperature (up to 40 °C) can improve sulfur removal by increasing the diffusion rate of oxidant radicals towards sulfur molecules and enhancing the mass transfer of aqueous $H_2O_2$ into the pores of the Pd/Zeolite catalyst. Elevated reaction temperatures can significantly enhance the oxidative desulfurization (ODS) process. By increasing the kinetic energy of reactant molecules and lowering the activation energy barrier, temperature elevation facilitates increased collision frequency and reaction rates. This is corroborated by the Arrhenius equation, which directly correlates the reaction rate constant with temperature and activation energy (Piao et al., 2021).

Experimental results demonstrate that increasing the temperature from 40 to 80 °C led to a substantial improvement in sulfur removal efficiency. This can be attributed to enhanced mass transfer and diffusion rates of reactants, as well as

improved interaction between sulfur compounds and the catalyst's active sites.However, excessive temperature increase beyond 80 °C can have detrimental effects. High temperatures may accelerate the decomposition of hydrogen peroxide ($H_2O_2$) into water, reducing the concentration of active peroxy species and hindering the oxidation process (Dizaji et al., 2019).

As illustrated in Figures 4.11a, 4.11b, and 4.11c, there is a clear correlation between sulfur conversion and oxidation temperature. The highest sulfur removal efficiency of 93.11% was achieved at 80 °C, 1.2 Hz, and a 12-minute residence time.The experimental data also indicates that increasing the oscillation frequency significantly improves sulfur conversion by enhancing mass and heat transfer within the OBR. This improvement is attributed to the formation of larger vortices during flow reversal and an extended eddy detachment length from the baffles. Baffles play a crucial role in the design of an oscillatory reactor by promoting efficient mixing and mass transfer.

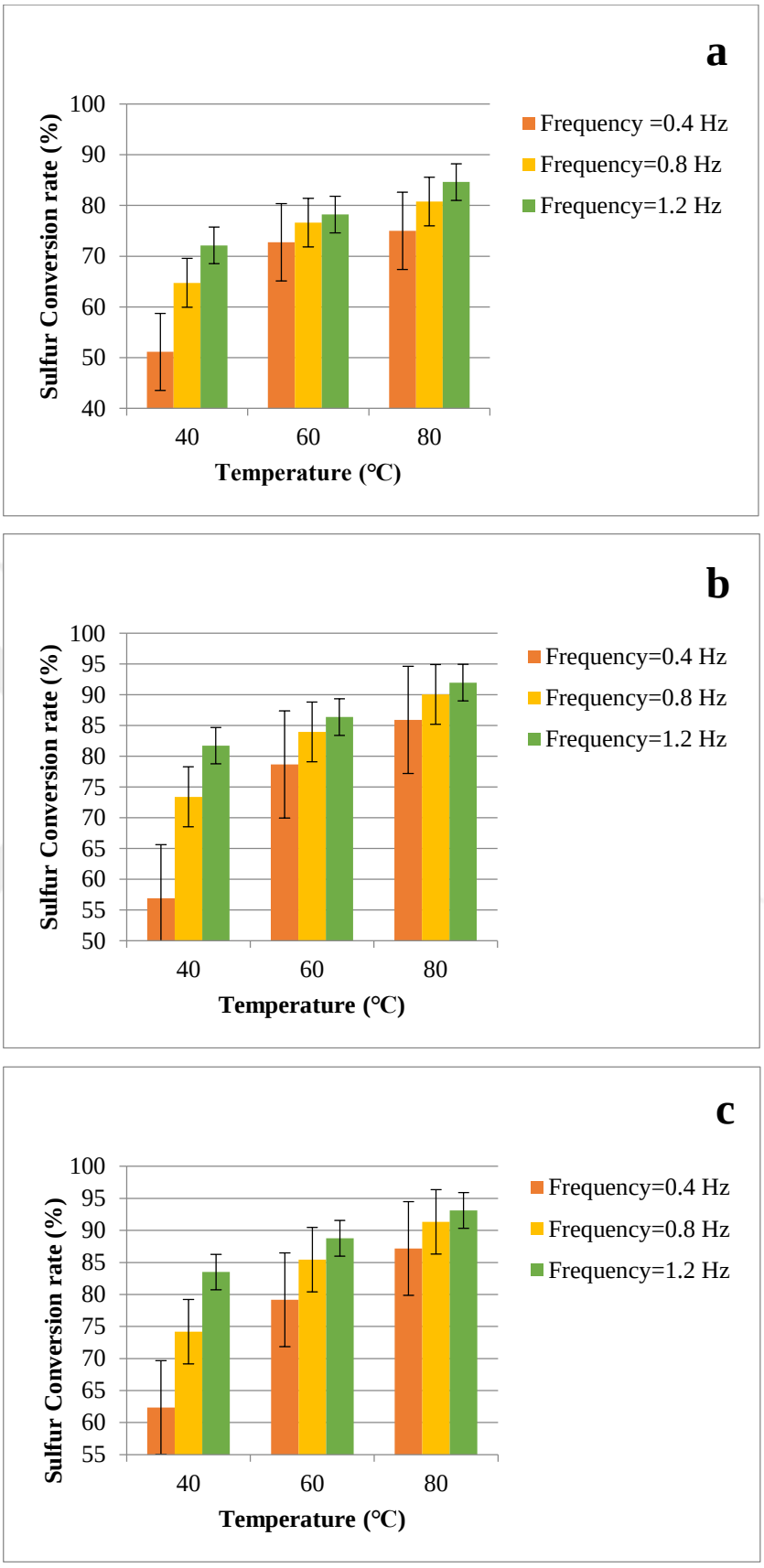


**Figure 4.2.** Impact of reaction temperature on sulfur removal using the catalyst (Pd/Zeolite) at: (a) τ = 4 min, (b) τ = 8 min, (c) τ = 12 min.

### 4.3.3 Impact of Oscillatory Frequency on OBR Sulfur Removal

The study focused on optimizing mixing conditions in the oscillatory baffle reactor (OBR) by investigating the removal of sulfur from light gas oil. This was analyzed as a function of oscillation frequency (0.4, 0.8, and 1.2 Hz), and varying residence times (4, 8, and 12 minutes), with the temperatures of reaction (40, 60, and 80 °C). The experiments utilized a catalyst of 0.15 mg (Pd/Zeolite) and 2 ml of $H_2O_2$ as the oxidant, conducted at 1 atm. The experimental findings indicated that the oscillatory frequency significantly influenced the oxidative desulfurization process. The observed rise in oscillation frequency from f = 0.4-1.2 Hz correlates with an enhanced efficiency of sulfur removal, as illustrated in Figure 4.12a, b, c.

As depicted in Figure 4.12a and 4.12b, a clear correlation exists between sulfur conversion and oscillation frequency. Increasing the frequency from 0.4 Hz to 0.8 Hz at 40 °C and a 4-minute residence time led to a significant increase in sulfur conversion from 44.71% to 58.33%. Further increasing the frequency to 1.2 Hz resulted in a conversion of 65.71% under the same conditions. Similarly, at 60 °C and an 8-minute residence time, increasing the frequency from 0.4 Hz to 0.8 Hz improved sulfur removal from 82.53% to 87.18%, and to 88.94% at 1.2 Hz. Because the OBR is better at transferring mass and heat, the sulfur conversion enhanced as the oscillation frequency increases. Higher frequencies lead to larger vortices during flow reversal and extended eddy detachment lengths from the baffles, facilitating better mixing and contact between reactants and the catalyst.

The enhancement of the ODS process by increasing the oscillation frequency from 0.4 to 0.8 Hz resulted in improved sulfur removal, rising from 86.06% to 91.35% at a reaction temperature of 80 °C and $\tau$ of 12 min. Figure 4.12c illustrates that optimal removal was achieved by maintaining constant conditions while increasing the oscillation frequency to 1.2 Hz, resulting in an enhanced sulfur removal rate of 93.11%, as depicted in the figure.

The frequency of oscillation is defined as the number of oscillations occurring per second (Abbott et al., 2013b). The findings indicated that a sufficient oscillation frequency is essential for enhancing the conversion rate of sulfur removal from light gas oil. The increase in oscillation frequency improved conversion as a result of the local mixing intensity generated in the tubular reactor (McDonough et al., 2019). The baffles enhanced the vortices along the reactor's length, improving radial dispersion, which facilitated the uniform suspension and

conveyance of solids within the tubular reactor. Consequently, this led to increased mass transfer and heat transfer (McDonough et al., 2015b). An increase in oscillation frequency results in a higher overall mass transfer coefficient (KLa) in the oscillatory baffle reactor (Hewgill et al., 1993; Humadi et al., 2022). Therefore, the mass transfer rate of the oxidant with sulfur in light gas oil was improved. The dispersion of $H_2O_2$ molecules in the light gas oil phase is improved, helping the fast transfer of radicals (•OH) that interact with sulfur within the catalyst's porosity, resulting in its conversion to sulfoxide and sulfone (Humadi et al., 2022).

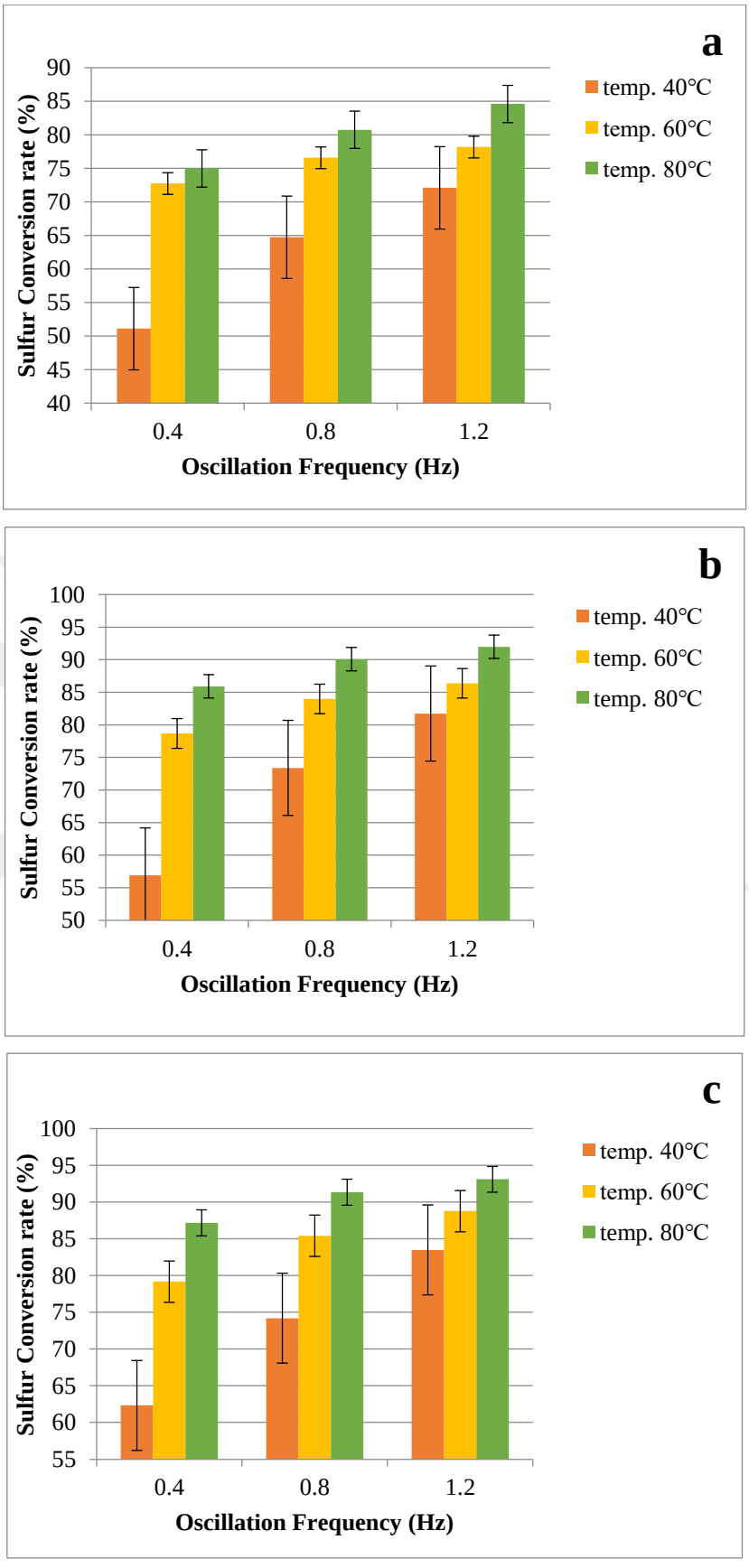


**Figure 4.3.** Effect of oscillation Frequency on sulfur removal using the catalyst (Pd/Zeolite) at: (a) τ = 4 min, (b) τ = 8 min, (c) τ = 12 min.

The results of the present work can be compared with some previous studies that have been collected and have similar or close operating conditions to the present study as shown in the Table 4.1.

**Table 4.1.** Present work compared with previous studies

| **Feedstock-sulfur type** | **Reactor** | **Catalyst /oxidant** | **Temp. (°C)** | **Time (min)** | **Freq. (Hz)** | **Conversion (%)** | **Ref.** |
|---|---|---|---|---|---|---|---|
| Model fuel-DBT | Stirrer Batch reactor | (Mo/HY-Zeolite)/ $H_2O_2$ | 60 | 90 | - | 90 | (Dadashi et al., 2020) |
| Light gas oil-DBT | Batch reactor | (AgO/ZnO/HY-zeolite)/ Air | 160 | 60 | - | 91.8 | (Abdulateef et al., 2021) |
| Light gas oil- different sulfur compounds | Digital baffle batch reactor | (CuO/AC)/ $H_2O_2$ | 140 | 45 | - | 83.1 | (Hameed et al., 2023b) |
| Diesel fuel-DBT | Meso OBR | Acetic acid/$H_2O_2$ | 80 | 3 | 4 | 94 | (Humadi et al., 2022) |
| Light gas oil- different sulfur compounds | OBR | (Pd/Zeolite)/ $H_2O_2$ | 80 | 12 | 1.2 | 93.11 | Present study |

### 4.3.4 Proposed Mechanism for Oxidative Desulfurization of Light Gas Oil

A possible mechanism for the oxidative desulfurization (ODS) process using hydrogen peroxide and a Pd/Zeolite catalyst in an oscillatory baffle reactor as shown in Figure 4.4. involves three main stages:

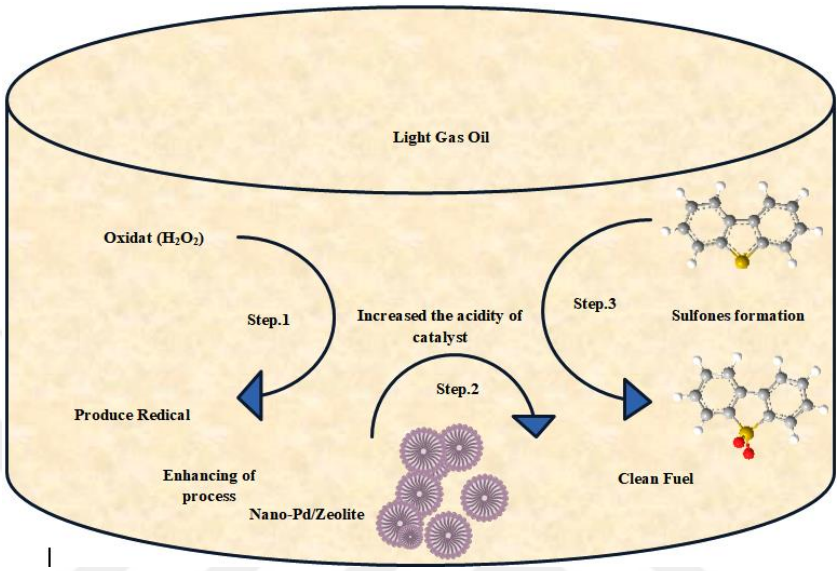


**Figure 4.4.** Chemical reaction mechanism for the oxidation desulfurization process.

1. **Adsorption:** Dibenzothiophene (DBT) molecules are initially adsorbed onto the surface of the Pd/Zeolite catalyst through physical or chemical interactions.
2. **Oxidation:** The adsorbed DBT molecules are oxidized by reactive oxygen species generated from the decomposition of hydrogen peroxide on the catalyst surface. Palladium plays a crucial role in activating hydrogen peroxide and facilitating the formation of these reactive oxygen species. The oxidation process converts DBT into its corresponding sulfoxide (DBTO).
3. **Further Oxidation:** The formed DBTO can be further oxidized to DBT sulfone ($DBTO_2$) in the presence of excess oxygen.

This proposed mechanism highlights the synergistic effect of adsorption and oxidation processes, facilitated by the unique properties of the Pd/Zeolite catalyst and the oscillatory flow conditions in the reactor.

# 5. CONCLUSION

A novel heterogeneous catalyst design (Pd/Zeolite) has been developed using the incipient Wetness Impregnation (IWI) method, using ($H_2O_2$) as an oxidant to enhance the oxidative desulfurization process (ODS). This was achieved through a newly novel piloting plant design of an oscillation baffled reactor (OBR) involving helical baffles. The recently developed catalyst has undergone characterization through FTIR, XRD, BET, TGA, FESEM, and EDX tests, which shows high efficiency. The oxidative desulfurization process of the (Pd/Zeolite) is significantly influenced by the porocity of the support, which is crucial for preserving the large surface area of the (Pd/Zeolite) following the incorporation of the palladium oxide (i.e. active compounds).

The parameters examined encompassed a variety of ranges, including temperature (40, 60, 80 ◦C), residence time (4, 8, 12 min), and oscillatory frequency (0.4, 0.8, 1.2 Hz), all conducted at 1 atm. The catalyst (Pd/Zeolite) demonstrated superior adsorption capabilities for organic sulfur content, achieving a sulfur conversion rate of 93.11%, marking the maximum conversion of sulfur. This was accomplished at a the temperature reaction of 80 ◦C, with a duration of 12 minutes and a frequency of 1.2 Hz, representing the peak values observed in this parametric investigation. The catalyst demonstrates outstanding desulfurization capabilities, resulting in superior performance for the ODS process attributed to the abundant active sites present in the synthesized catalyst structure. The interaction between the metal oxide (Palladium oxide) and the mesoporous support (Zeolite) may facilitate the transfer of sulfur molecules from the liquid fuel to the catalyst via the porous structure within the ODS.

A reactor design that uses piloting plant oscillation baffles efficiently conduct the heterogeneous ODS process. Even at low operating conditions, the catalyst, oxidant, and sulfur compounds in light gas oil were thoroughly mixed thanks to the reactor's oscillating helical baffled design. The results showed that sulfur was significantly removed in just 12 minutes of reaction time, which is in contrast to the long residence durations seen in standard reactor types used for oxidative desulfurization (ODS), such as batch reactors and trickling bed reactors.

## 5.1 Recommendations

To further optimize the oxidative desulfurization (ODS) process and expand its application, the following recommendations are proposed:

1. **Catalyst Optimization:**
    - Investigate the impact of varying metal loadings of cobalt and manganese on catalyst activity and selectivity.
    - Explore alternative synthesis techniques, such as sol-gel, flame hydrolysis, and ion exchange, to produce catalysts with improved properties.
2. **Reactor Design and Operation:**
    - Conduct a comparative study of different baffle designs (orifice, multi-orifice, central, and integral) in OBRs to assess their impact on mixing patterns, mass transfer, and overall ODS performance.
    - Investigate the influence of reactor geometry, including tube diameter, baffle open area, spacing, thickness, and diameter, on the efficiency of the ODS process.
    - Explore the potential of trickle bed reactors (TBRs) with improved feed distribution to mitigate channeling effects and enhance reactor performance.
3. **Process Optimization:**
    - Conduct a comprehensive study to optimize reaction parameters, such as temperature, pressure, residence time, and oxidant concentration, to maximize sulfur removal efficiency.
    - Investigate the use of alternative oxidants and solvents to improve the economic and environmental sustainability of the ODS process.

By addressing these recommendations, future research can contribute to the development of more efficient and sustainable ODS technologies, ultimately leading to cleaner and higher-quality fuels.

# REFERENCES


A Review on Desulfurization Techniques of Liquid Fuels. (2016). *International Journal of Science and Research (IJSR)*, *5*(5), 2413–2419. https://doi.org/10.21275/v5i5.nov164036

Abbas, G., Kumar, N., Kumar, D., & Pandey, G. (2019). Effect of reaction temperature on shape evolution of palladium nanoparticles and their cytotoxicity against A-549 lung cancer cells. *ACS Omega*, *4*(26), 21839–21847.

Abbas, M. N., & Ibrahim, S. A. (n.d.). *Catalytic and thermal desulfurization of light naphtha fraction, JKSUES 32 (2020) 229e235*.

Abbott, M. S. R., Harvey, A. P., Perez, G. V., & Theodorou, M. K. (2013a). Biological processing in oscillatory baffled reactors: operation, advantages and potential. *Interface Focus*, *3*(1), 20120036.

Abbott, M. S. R., Harvey, A. P., Perez, G. V., & Theodorou, M. K. (2013b). Biological processing in oscillatory baffled reactors: operation, advantages and potential. *Interface Focus*, *3*(1), 20120036. https://doi.org/10.1098/rsfs.2012.0036

Abdulateef, L. T., Nawaf, A. T., Al-Janabi, O. Y. T., Foot, P. J. S., & Mahmood, Q. A. (2021). Batch Oxidative Desulfurization of Model Light Gasoil over a Bimetallic Nanocatalyst. *Chemical Engineering & Technology*, *44*(9), 1708–1715. https://doi.org/10.1002/ceat.202100027

Adam, M., Anbari, H., Hart, A., Wood, J., Robinson, J. P., & Rigby, S. P. (2021). In-situ microwave-assisted catalytic upgrading of heavy oil: Experimental validation and effect of catalyst pore structure on activity. *Chemical Engineering Journal*, *413*, 127420.

Aida, T. (1998). *Process for recovering organic sulphur compounds from fuel oil, U.S. Patent 5*.

Aida, T., & Funakoshi, I. (1993). *Method of recovering organic sulfur compound from liquid oil*. 10–13.

Akopyan, A., Eseva, E., Polikarpova, P., Kedalo, A., Vutolkina, A., & Glotov, A. (2020). Deep Oxidative Desulfurization of Fuels in the Presence of Brönsted Acidic Polyoxometalate-Based Ionic Liquids. *Molecules*, *25*(3), 536. https://doi.org/10.3390/molecules25030536

Al-Malki, A. (2004). *Desulfurization of gasoline and diesel fuels, using non-hydrogen consuming techniques*. King Fahd University of Petroleum and Minerals (Saudi Arabia).

Ali, M. F., Al-Malki, A., & Ahmed, S. (2009). Chemical desulfurization of petroleum fractions for ultra-low sulfur fuels. *Fuel Processing Technology*, *90*(4), 536–544. https://doi.org/10.1016/j.fuproc.2009.01.005

Anderson, C. J., Harris, M. C., & Deglon, D. A. (2009). Flotation in a novel oscillatory baffled column. *Minerals Engineering*, *22*(12), 1079–1087.

Argyle, M. D., & Bartholomew, C. H. (2015). Heterogeneous catalyst deactivation and regeneration: a review. *Catalysts*, *5*(1), 145–269.

ARP. (2010). Acid Rain Program | Clean Air Markets | US Environmental Protection Agency. *Epa*. http://www.epa.gov/airmarkets/programs/arp/

Avila, M., Kawas, B., Fletcher, D. F., Poux, M., Xuereb, C., & Aubin, J. (2022). Design, performance characterization and applications of continuous oscillatory baffled reactors. *Chemical Engineering and Processing-Process Intensification*, *180*, 108718.

Azarpour, A., Rezaei, N., & Zendehboudi, S. (2021). Performance analysis and modeling of catalytic trickle-bed reactors: A comprehensive review. *Journal of Industrial and Engineering Chemistry*, *103*, 1–41.

Babich, I. V., & Moulijn, J. A. (2003). Science and technology of novel processes for deep desulfurization of oil refinery streams: A review. *Fuel*, *82*(6), 607–631. https://doi.org/10.1016/S0016-2361(02)00324-1

Bagherzadeh, M., & Amini, M. (2009). Synthesis, characterization and catalytic study of a novel iron(III)-tridentate Schiff base complex in sulfide oxidation by UHP. *Inorganic Chemistry Communications*, *12*(1), 21–25. https://doi.org/10.1016/j.inoche.2008.10.023

Beshkoofeh, S., Ghalami-Choobar, B., Shahidian, Z., & Khosharay, S. (2021). Preparation, characterization, and kinetics model of MoCo/γ-Al2O3 catalysts for oxidative desulfurization of light naphtha. *Iranian Journal of Chemistry and Chemical Engineering*, *40*(6), 1777–1792.

Bhadra, B. N., & Jhung, S. H. (2019). Oxidative desulfurization and denitrogenation of fuels using metal-organic framework-based/-derived catalysts. *Applied Catalysis B: Environmental*, *259*, 118021. https://doi.org/10.1016/j.apcatb.2019.118021

Blanco-Brieva, G., Campos-Martin, J. M., Al-Zahrani, S. M., & Fierro, J. L. G. (2010). Removal of refractory organic sulfur compounds in fossil fuels using mof sorbents. *Global Nest Journal*, *12*(3), 296–304. https://doi.org/10.30955/gnj.000721

C. Song. (2013). An overview of new approaches to deep desulfurization for ultra-clean gasoline, diesel fuel and jet fuel. *Catalysis Today*, *86*, 211–263.

Campos-Martin, J. M., & Capel-Sanchez, M. C. (2021). Catalytic oxidative desulfurization of liquid fuels. In *Catalytic and noncatalytic upgrading of oils* (pp. 143–174). ACS Publications.

Čejka, J., Centi, G., Perez-Pariente, J., & Roth, W. J. (2012). Zeolite-based materials for novel catalytic applications: Opportunities, perspectives and open problems. *Catalysis Today*, *179*(1), 2–15.

Chen, T.-C., Shen, Y.-H., Lee, W.-J., Lin, C.-C., & Wan, M.-W. (2013). An economic analysis of the continuous ultrasound-assisted oxidative desulfurization process applied to oil recovered from waste tires. *Journal of Cleaner Production*, *39*, 129–136. https://doi.org/10.1016/j.jclepro.2012.09.001

Cheng, S. S. (2008). *Ultra clean fuels via modified UAOD process with room temperature ionic liquid (RTIL) & solid catalyst polishing*. University of Southern California.

Choeichom, P., & Sirivat, A. (2018). Discriminative sensing performances of ZSM-5, Y, mordenite, ferrierite, beta, 3A, 4A, 5A, and 13X zeolites towards sulfur dioxide. *Ionics*, *24*, 2829–2841.

Choi, M., Wu, Z., & Iglesia, E. (2010). Mercaptosilane-assisted synthesis of metal clusters within zeolites and catalytic consequences of encapsulation. *Journal of the American Chemical Society*, *132*(26), 9129–9137.

Dadashi, M., Mazloom, G., Akbari, A., & Banisharif, F. (2020). The performance of micro-meso-pore HY zeolite for supporting Mo toward oxidation of dibenzothiophene. *Environmental Science and Pollution Research*, *27*, 30600–30614.

Dardouri, R., Gannouni, A., & Zina, M. S. (2019). Structural and Oxidative Properties of Manganese Incorporated Mesostructure Silica for Methane Oxidation. *Advances in Materials Science and Engineering*, *2019*. https://doi.org/10.1155/2019/6024876

Di Giuseppe, A., Crucianelli, M., De Angelis, F., Crestini, C., & Saladino, R. (2009). Efficient oxidation of thiophene derivatives with homogeneous and heterogeneous MTO/H2O2 systems: A novel approach for, oxidative desulfurization (ODS) of diesel fuel. *Applied Catalysis B: Environmental*, *89*(1–2), 239–245. https://doi.org/10.1016/j.apcatb.2009.02.009

Dizaji, A. K., Mokhtarani, B., & Mortaheb, H. R. (2019). Deep and fast oxidative desulfurization of fuels using graphene oxide-based phosphotungstic acid catalysts. *Fuel*, *236*, 717–729. https://doi.org/10.1016/j.fuel.2018.09.076

Folsom, B. R., Schieche, D. R., DiGrazia, P. M., Werner, J., & Palmer, S. (1999). Microbial desulfurization of alkylated dibenzothiophenes from a hydrodesulfurized middle distillate by Rhodococcus erythropolis I-19. *Applied and Environmental Microbiology*, *65*(11), 4967–4972. https://doi.org/10.1128/aem.65.11.4967-4972.1999

Foutch, G. L., & Johannes, A. H. (2003). Reactors in process engineering. *Encyclopedia of Physical Science and Technology*, *1*, 1–54.

Gao, Y., Gao, R., Zhang, G., Zheng, Y., & Zhao, J. (2018). Oxidative desulfurization of model fuel in the presence of molecular oxygen over polyoxometalate based catalysts supported on carbon nanotubes. *Fuel*, *224*, 261–270. https://doi.org/10.1016/j.fuel.2018.03.034

Gheni, S. A., Jarullah, A. T., & Razak, G. H. A. (2017). OXIDATIVE CATALYTIC DESULPHURIZATION OF NAPHTHA IN A TRICKLE BED REACTOR. *Petroleum & Coal*, *59*(2).

Gokhale, S., & Khare, M. (2004). A review of deterministic, stochastic and hybrid vehicular exhaust emission models. *International Journal of Transport Management*, *2*(2), 59–74.

Groysman, A. (2017). *Corrosion problems and solutions in oil refining and petrochemical industry* (Vol. 61). Springer.

Hameed, S. A., Nawaf, A. T., Mahmood, Q. A., Abdulateef, L. T., Jarullah, A. T., & Mujtaba, I. M. (2023a). Production of Green Fuel: A Digital Baffle Batch Reactor for Enhanced Oxidative Desulfurization of Light Gas Oil Using Nano-Catalyst. *Iran. J. Chem. Chem. Eng. Research Article Vol*, *42*(3).

Hameed, S. A., Nawaf, A. T., Mahmood, Q. A., Abdulateef, L. T., Jarullah, A. T., & Mujtaba, I. M. (2023b). Production of Green Fuel: A Digital Baffle Batch Reactor for Enhanced Oxidative Desulfurization of Light Gas Oil Using Nano-Catalyst. *Iranian Journal of Chemistry and Chemical Engineering*, *42*(3), 740–753. https://doi.org/10.30492/IJCCE.2022.547416.5138

Hern, C., Fulfillment, P., & For, R. (2020). *Modeling of Sulfur Removal from Heavy Fuel Oil Using Ultrasound-Assisted Oxidative Desulfurization Thesis by*. *June*.

Hewgill, M. R., Mackley, M. R., Pandit, A. B., & Pannu, S. S. (1993). Enhancement of gas-liquid mass transfer using oscillatory flow in a baffled tube. *Chemical Engineering Science*, *48*(4), 799–809. https://doi.org/10.1016/0009-2509(93)80145-G

Horii, Y., Onuki, H., Doi, S., Mori, T., Takatori, T., Sato, H., Ookuro, T., & Sugawara, T. (1993). Desulfurization and denitration of light oil by extraction. *US Patent*, *5*, 494, 572. http://www.google.com/patents/US5494572%5Cnhttp://patentimages.storage.googleapis.com/pdfs/US5494572.pdf

Houda, S., Lancelot, C., Blanchard, P., Poinel, L., & Lamonier, C. (2018). Oxidative desulfurization of heavy oils with high sulfur content: A review. *Catalysts*, *8*(9), 344.

Huirache-Acuña, R., Pawelec, B., Loricera, C. V., Rivera-Muñoz, E. M., Nava, R., Torres, B., & Fierro, J. L. G. (2012). Comparison of the morphology and HDS activity of ternary Ni(Co)-Mo-W catalysts supported on Al-HMS and Al-SBA-16 substrates. *Applied Catalysis B: Environmental*, *125*, 473–485. https://doi.org/10.1016/j.apcatb.2012.05.034

Humadi, J. I., Gheni, S. A., Ahmed, S. M. R., Abdullah, G. H., Phan, A. N., & Harvey, A. P. (2021). Fast, non-extractive, and ultradeep desulfurization of diesel in an oscillatory baffled reactor. *Process Safety and Environmental Protection*, *152*, 178–187. https://doi.org/10.1016/j.psep.2021.05.028

Humadi, J. I., Gheni, S. A., Ahmed, S. M. R., & Harvey, A. (2022). Dimensionless evaluation and kinetics of rapid and ultradeep desulfurization of diesel fuel in an oscillatory baffled reactor. *RSC Advances*, *12*(23), 14385–14396. https://doi.org/10.1039/D2RA01663J

Ismagilov, Z., Yashnik, S., Kerzhentsev, M., Parmon, V., Bourane, A., Al-Shahrani, F. M., Hajji,

A. A., & Koseoglu, O. R. (2011). Oxidative Desulfurization of Hydrocarbon Fuels. *Catalysis Reviews*, *53*(3), 199–255. https://doi.org/10.1080/01614940.2011.596426

ISODA, D. (1998). Challenges in the hydrodesulfurization of polyaromatic sulfur compounds. *Adv. Catal*, *42*(345), 60631–60638.

Jarullah, A. T., Aldulaimi, S. K., Al-Tabbakh, B. A., & Mujtaba, I. M. (2020). A new synthetic composite nano-catalyst achieving an environmentally Friendly fuel by batch oxidative desulfurization. *Chemical Engineering Research and Design*, *160*, 405–416.

Jian, H., & Ni, X. (2005). A numerical study on the scale-up behaviour in oscillatory baffled columns. *Chemical Engineering Research and Design*, *83*(10), 1163–1170.

Jose, N., Sengupta, S., & Basu, J. K. (2011). Optimization of oxidative desulfurization of thiophene using Cu/titanium silicate-1 by box-behnken design. *Fuel*, *90*(2), 626–632.

Kilbane, J. J. (2017). Biodesulfurization: how to make it work? *Arabian Journal for Science and Engineering*, *42*(1), 1–9.

Kim, D. J., & Chung, H. S. (2003). Synthesis and characterization of ZSM-5 zeolite from serpentine. *Applied Clay Science*, *24*(1–2), 69–77.

Laybourn, A., López-Fernández, A. M., Thomas-Hillman, I., Katrib, J., Lewis, W., Dodds, C., Harvey, A. P., & Kingman, S. W. (2019). Combining continuous flow oscillatory baffled reactors and microwave heating: Process intensification and accelerated synthesis of metal-organic frameworks. *Chemical Engineering Journal*, *356*, 170–177.

Liu, D., Yakshimuradova, J., Forest, R., Knopf, F. C., & Dooley, K. (2010). Catalytic oxidative desulfurization of model diesel. *AIChE Annual Meeting, Conference Proceedings*.

Liu, Y., Lai, Q., Sun, Y., Xu, X., Fang, X., Liu, Y., Rao, C., & Wang, X. (2019). SnO2/Al2O3 catalysts for selective reduction of NOx by propylene: on the promotional effects of plasma treatment in air atmosphere. *Catalysis Today*, *337*, 171–181.

McDonough, J. R., Oates, M. F., Law, R., & Harvey, A. P. (2019). Micromixing in oscillatory baffled flows. *Chemical Engineering Journal*, *361*, 508–518. https://doi.org/10.1016/j.cej.2018.12.088

McDonough, J. R., Phan, A. N., & Harvey, A. P. (2015a). Rapid process development using oscillatory baffled mesoreactors–A state-of-the-art review. *Chemical Engineering Journal*, *265*, 110–121.

McDonough, J. R., Phan, A. N., & Harvey, A. P. (2015b). Rapid process development using oscillatory baffled mesoreactors – A state-of-the-art review. *Chemical Engineering Journal*, *265*, 110–121. https://doi.org/10.1016/j.cej.2014.10.113

Mehrabadi, B. A. T., Eskandari, S., Khan, U., White, R. D., & Regalbuto, J. R. (2017). A review of preparation methods for supported metal catalysts. *Advances in Catalysis*, *61*, 1–35.

Mohammed, A. E., Mohammed, W. T., & Gheni, S. A. (2024). Environmental benefits of Agricultural Waste-Derived catalysts in diesel Desulfurization: A review. *Cleaner Materials*, 100262.

Mohammed, H. R., Gheni, S. A., Hamad, K. I., Ahmed, S. M. R., Habeeb, O. A., & Mahmood, M. A. (2022). Synthesis, evaluation, and optimal stability of a biowaste-based catalytic oxidative desulfurization of model fuel in a trickle bed reactor. *Process Safety and Environmental Protection*, *163*, 513–527.

Moliner, M., Martínez, C., & Corma, A. (2015). Multipore zeolites: synthesis and catalytic applications. *Angewandte Chemie International Edition*, *54*(12), 3560–3579.

Monticello, D. J. (2000). Biodesulfurization and the upgrading of petroleum distillates. *Current Opinion in Biotechnology*, *11*(6), 540–546. https://doi.org/10.1016/S0958-1669(00)00154-3

Nanoti, A., Dasgupta, S., Agnihotri, V., Gupta, P., Goswami, A. N., Garg, M. O., Tangstad, E., Stöcker, M., Karlsson, A., & Vistad, Ø. B. (2011). A zeolite based vapor phase adsorptive desulfurization process for naphtha. *Microporous and Mesoporous Materials*, *146*(1–3), 158–165. https://doi.org/10.1016/j.micromeso.2011.01.009

Nawaf, A. T. (2015). *Experimental and modeling study for desulfurization of light gas oil by catalytic wet air oxidation process*. MSc. thesis, Tikrit University, Iraq.

Nawaf, A. T., Jarullah, A. T., & Abdulateef, L. T. (2019). Design of a synthetic zinc oxide catalyst over nano-alumina for sulfur removal by air in a batch reactor. *Bulletin of Chemical Reaction Engineering & Catalysis*, *14*(1), 79.

Ni, X.-W. (2006). Continuous oscillatory baffled reactor technology. *Innovations in Pharmaceutical Technology*, *20*, 90–96.

Ni, X., Brogan, G., Struthers, A., Bennett, D. C., & Wilson, S. F. (1998). A systematic study of the effect of geometrical parameters on mixing time in oscillatory baffled columns. *Chemical Engineering Research and Design*, *76*(5), 635–642.

Nigam, K. D. P., & Larachi, F. (2005). Process intensification in trickle-bed reactors. *Chemical Engineering Science*, *60*(22), 5880–5894.

Ogunlaja, A. S. (2013). *Oxidative Desulfurization of Fuel Oils-Catalytic Oxidation and Adsorptive Removal of Organosulfur Compounds*. *December*, 310.

Otaghsaraei, S. S., Kazemeini, M., Hasannia, S., & Ekramipooya, A. (2022). Deep oxidative desulfurization via rGO-immobilized tin oxide nanocatalyst: Experimental and theoretical perspectives. *Advanced Powder Technology*, *33*(3), 103499.

Otsuki, S., Nonaka, T., Takashima, N., Qian, W., Ishihara, A., Imai, T., & Kabe, T. (2000). Oxidative Desulfurization of Light Gas Oil and Vacuum Gas Oil by Oxidation and Solvent Extraction. *Energy & Fuels*, *14*(6), 1232–1239. https://doi.org/10.1021/ef000096i

Pérez-Ramírez, J., Christensen, C. H., Egeblad, K., Christensen, C. H., & Groen, J. C. (2008). Hierarchical zeolites: enhanced utilisation of microporous crystals in catalysis by advances in materials design. *Chemical Society Reviews*, *37*(11), 2530–2542.

Phan, A. N., & Harvey, A. P. (2012). Characterisation of mesoscale oscillatory helical baffled reactor—Experimental approach. *Chemical Engineering Journal*, *180*, 229–236.

Phan, A. N., Harvey, A. P., & Eze, V. (2012). Rapid production of biodiesel in mesoscale oscillatory baffled reactors. *Chemical Engineering & Technology*, *35*(7), 1214–1220.

Phan, A. N., Harvey, A. P., & Rawcliffe, M. (2011a). Continuous screening of base-catalysed biodiesel production using new designs of mesoscale oscillatory baffled reactors. *Fuel Processing Technology*, *92*(8), 1560–1567.

Phan, A. N., Harvey, A. P., & Rawcliffe, M. (2011b). Continuous screening of base-catalysed biodiesel production using New designs of mesoscale oscillatory baffled reactors. *Fuel Processing Technology*, *92*(8), 1560–1567. https://doi.org/10.1016/j.fuproc.2011.03.022

Piao, W., Li, Z., Li, C., Park, J. S., Lee, J., Li, Z., Kim, K. Y., Jin, L. Y., Kim, J. M., & Jin, M. (2021). Efficient and reusable ordered mesoporous WO x/SnO 2 catalyst for oxidative desulfurization of dibenzothiophene. *RSC Advances*, *11*(44), 27453–27460.

Piva, D. H., Piva, R. H., Picinini, M., Rodrigues, A. D., & Urquieta-González, E. A. (2021). Correlation between structural evolution and oxidative desulfurization activity for magnetically-recoverable γ-Fe2O3@ SiO2 core-shell–Supported WOx nanostructure. *Catalysis Communications*, *148*, 106182.

Primo, A., & Garcia, H. (2014). Zeolites as catalysts in oil refining. *Chemical Society Reviews*, *43*(22), 7548–7561.

Rajendran, A., Cui, T., Fan, H., Yang, Z., Feng, J., & Li, W. (2020). A comprehensive review on oxidative desulfurization catalysts targeting clean energy and environment. *Journal of Materials Chemistry A*, *8*(5), 2246–2285. https://doi.org/10.1039/C9TA12555H

Rezvani, M. A., Afshari, P., & Aghmasheh, M. (2021). Deep catalytic oxidative desulfurization process catalyzed by TBA-PWFe@NiO@BNT composite material as an efficient and recyclable phase-transfer nanocatalyst. *Materials Chemistry and Physics*, *267*, 124662. https://doi.org/10.1016/j.matchemphys.2021.124662

Richardson, J. T. (2013). *Principles of catalyst development*. Springer.

Rivera, J. L., Navarro-Santos, P., Guerra-Gonzalez, R., & Lima, E. (2014). Interaction of Refractory Dibenzothiophenes and Polymerizable Structures. *International Journal of Polymer Science*, *2014*, 1–11. https://doi.org/10.1155/2014/103945

Saleh, T. A. (2020). Characterization, determination and elimination technologies for sulfur from petroleum: toward cleaner fuel and a safe environment. Trends Environ Anal Chem 25: e00080. *Doi. Org/10.1016/j. Teac*, e0008.

Sanyangare, F. (2016). *Simulation of the Adsorptive Desulphurisation of Diesel Fuel*. *1075399*.

Sarda, K. K., Bhandari, A., Pant, K. K., & Jain, S. (2012). Deep desulfurization of diesel fuel by selective adsorption over Ni/Al2O3 and Ni/ZSM-5 extrudates. *Fuel*, *93*, 86–91. https://doi.org/10.1016/j.fuel.2011.10.020

Shafi, R., & Hutchings, G. J. (2000). Hydrodesulfurization of hindered dibenzothiophenes: an overview. *Catalysis Today*, *59*(3–4), 423–442. https://doi.org/10.1016/S0920-5861(00)00308-4

Shafiq, I., Shafique, S., Akhter, P., Ishaq, M., Yang, W., & Hussain, M. (2021). Recent breakthroughs in deep aerobic oxidative desulfurization of petroleum refinery products. *Journal of Cleaner Production*, *294*, 125731.

Sharifi, K., Halladj, R., Royaee, S. J., & Nasr, M. R. J. (2018). A new approach for gasoline upgrading: Coupling octane enhancement and desulfurization of heavy straight-run naphtha over Ni/HZSM-5 catalyst. *Catalysis Communications*, *115*, 31–35. https://doi.org/10.1016/j.catcom.2018.07.005

Sharifi, K., Halladj, R., Royaee, S. J., & Nasr, M. R. J. (2019). Investigation of the effect of HZSM-5 over HDS and reforming processes for clean gasoline production. *International Journal of Environmental Science and Technology*, *16*, 865–874.

Shiflett, W. K., & Krenzke, L. D. (2002). Consider improved catalyst technologies to remove sulfur. *Hydrocarbon Processing*, *81*(2), 41–43.

Silva, D. F., Viana, A. M., Mirante, F., de Castro, B., Cunha-Silva, L., & Balula, S. S. (2021). Removing Simultaneously Sulfur and Nitrogen from Fuel under a Sustainable Oxidative Catalytic System. *Sustainable Chemistry*, *2*(2), 382–391. https://doi.org/10.3390/suschem2020022

Song, C., & Ma, X. (2003). New design approaches to ultra-clean diesel fuels by deep desulfurization and deep dearomatization. *Applied Catalysis B: Environmental*, *41*(1–2), 207–238. https://doi.org/10.1016/S0926-3373(02)00212-6

Speight, J. G. (2000). The desulphurization of heavy gas oil and residue. *Marcel Dekker Inc.*

Tengco, J. M. M. (2016). *Synthesis of well dispersed supported metal catalysts by strong electrostatic adsorption and electroless deposition*. University of South Carolina.

Thomas, J. M., Raja, R., & Lewis, D. W. (2005). Single-site heterogeneous catalysts. *Angewandte Chemie International Edition*, *44*(40), 6456–6482.

Vellingiri, K., Deep, A., & Kim, K.-H. (2016). Metal–organic frameworks as a potential platform

for selective treatment of gaseous sulfur compounds. *ACS Applied Materials & Interfaces*, *8*(44), 29835–29857.

Wan, M.-W. (2006). *Development of a portable, modular unit for the optimization of ultrasound-assisted oxidative desulfurization of diesel*. University of Southern California.

Wang, H., Jibrin, I., & Zeng, X. (2020). Catalytic oxidative desulfurization of gasoline using phosphotungstic acid supported on MWW zeolite. *Frontiers of Chemical Science and Engineering*, *14*, 546–560.

Wang, H., Wang, L., & Xiao, F.-S. (2020). Metal@ zeolite hybrid materials for catalysis. *ACS Central Science*, *6*(10), 1685–1697.

Xia, D., Su, Y., & Qian, J. (1999). Study on the oxidation mechanism of mixed thiols in light oil sweetening. 3. Apparent kinetics of the catalytic cooxidation of mixed thiols in gas-liquid-solid systems. *Industrial and Engineering Chemistry Research*, *38*(4), 1291–1294. https://doi.org/10.1021/ie980541l

Xie, K., Jiang, B., Wang, Z., Zuo, S., & Wang, Q. (2023). Study on the performance and sulfur tolerance mechanism of Pd/beta zeolite in catalytic combustion of toluene. *Journal of Materials Research and Technology*, *25*, 4543–4553.

Zhang, Y., Fang, Z. Z., Sun, P., Xia, Y., Lefler, H. D., & Zheng, S. (2020). Deoxygenation of Ti metal. In *Extractive Metallurgy of Titanium* (pp. 181–223). Elsevier. https://doi.org/10.1016/B978-0-12-817200-1.00010-7

Zhao, D., Sun, F., Zhou, E., & Liu, Y. (2003). A review of desulfurization of light oil based on selective oxidation. *Shijiazhuang, China: College of Chemistry and Pharmaceutical Engineering, Hebei University of Science and Technology*.

Zhongming, Z., Linong, L., Xiaona, Y., Wangqiang, Z., & Wei, L. (2021). *EIA projects accelerating renewable consumption and steady liquid fuels growth to 2050*. https://doi.org/EIA projects accelerating renewable consumption and steady liquid fuels growth to 2050

# APPENDIX 1

## Laboratory calculations

The process of loading the active ingredient (Pd)

Here are the calculations for preparing 6 wt % of Pd on Zeolite:

$$wt\% = \frac{wt_{Pd}}{wt_{Pd} + wt_{Zeolite}} \times 100\%$$

$$3\% = \frac{X}{X+6} \times 100\% \quad \rightarrow \quad X = 0.06X + 0.36 = X$$

$$X - 0.06X = 0.36$$

$$X = \frac{0.36}{0.94} = 0.383\ gm\ of\ Pd$$

$$Weight\ of\ PdCl_2\ required \rightarrow wt = \frac{M.wt\ of\ PdCl_2}{M.wt\ of\ Pd} \times wt\ of\ Pd$$

$$wt = \frac{177.33}{106.4} \times 0.383 = 0.638\ gm\ of\ PdCl_2$$

# APPENDIX 2

The calculation of sulfur conversion was performed using the equation presented below:

$$\boldsymbol{Desulfurization\ efficiency} = \left[\frac{\boldsymbol{C_{in} - C_P}}{\boldsymbol{C_{in}}}\right] \times \mathbf{100}\%$$

Where:

$C_{in} = inlet\ sulfur\ concentration$

$C_P =\ \ product\ sulfur\ concentration$
$and\ the\ C_{in} = 624\ ppm.$

For the following values, which are typical for final-run calculations:

$C_{in} = 624\ ppm.$

$C_P = 43\ ppm.$

$$\boldsymbol{Desulfurization\ efficiency}(\%) = \left[\frac{\mathbf{624 - 43}}{\mathbf{624}}\right] \times \mathbf{100}$$

$$\boldsymbol{Desulfurization\ efficiency}(\%) = \mathbf{93.11}$$